

To my family

EIDESSTATTLICHE ERKLÄRUNG

Ich erkläre an Eides statt, dass ich die vorliegende Arbeit selbstständig verfasst, andere als die angegebenen Quellen/Hilfsmittel nicht benutzt, und die den benutzten Quellen wörtlich und inhaltlich entnommenen Stellen als solche kenntlich gemacht habe. Das in TUGRAZonline hochgeladene Textdokument ist mit der vorliegenden Dissertation identisch.

18.1.2016

Datum

Wendmüller S.

Unterschrift

Acknowledgements

As there are always people in the background, who helped in various ways during the creation of this work, I want to dedicate this page to them in order to thank them.

I want to thank my supervisor Prof. Dr. GÜNTER GRAMPP for providing guidance, helpful discussions and being available when needed.

I want to thank Prof. Dr. STEPHAN LANDGRAF for enlightening discussions and support when it was needed.

I want to thank Dr. KENNETH RASMUSSEN for helping me with small but still important things whenever he was here and for the detailed and helpful proofreading corrections, he did for me.

I want to thank JOSUA BÄCHLE, MSc for being a great colleague, creating a pleasant working atmosphere and for the helpful discussions of everyday problems.

I also want to thank the people of the institute, who see to it that everything runs smoothly, namely our secretary MARION HOFMEISTER, our lab assistant HILDE FREISSMUTH, HERBERT LANG and HELMUT EISENKÖLBL.

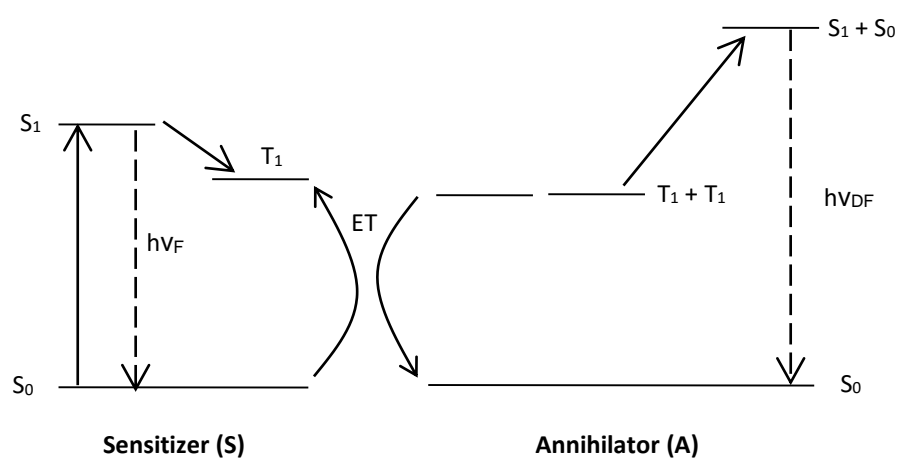
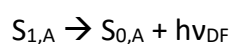
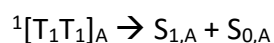
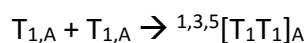
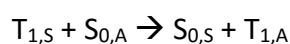
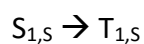
Finally I want to thank the FWF for funding with the FWF-ERANET project number I 931_N19

Thank You!

Abstract

Delayed Fluorescence is a well known process since the late 70s. It has been proved that an external magnetic field has an influence on the delayed fluorescence yield. Whereas this phenomenon has been studied extensively in the solid state, almost no experiments were done in solution. This work intends to explore the influence of the magnetic field on a process that leads to delayed fluorescence in solution.

The sensitized delayed fluorescence reaction can be summarized by the following equations:



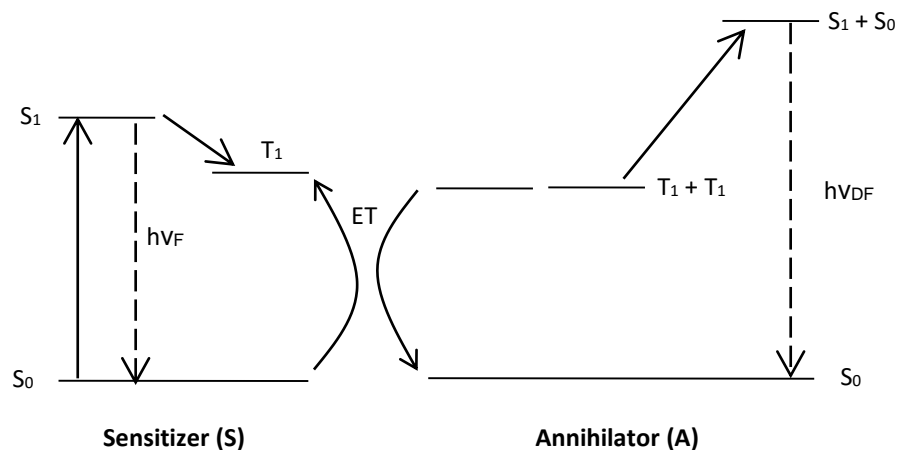
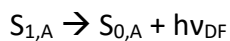
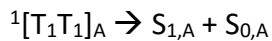
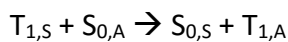
A magnetic field can influence the 4th reaction, as it splits the energy levels of triplet pairs, which can either be in singlet, triplet or quintet state. Whereas in a zero field situation all states are accessible, the number of attainable states in a high field situation differs.

The magnetic field effect on the lifetime and the intensity of different sensitizer/annihilator pairs in different solvents were studied. In the ZnTPP and Perylene system an additional emission, which does not belong to the normal delayed fluorescence, was observed. This signal shows a viscosity dependence that was analysed.

Zusammenfassung

Verzögerte Fluoreszenz ist seit den späten 70ern ein bekannter Prozess. Es wurde bewiesen, dass ein externes Magnetfeld einen Einfluss auf die Intensität der verzögerten Fluoreszenz hat. Während dieses Phänomen umfassend im festen Medium betrachtet wurde, gibt es fast keine Messungen in Lösung. Diese Arbeit hat die Intention den Einfluss eines Magnetfeldes auf den Prozess, welcher zu verzögerter Fluoreszenz führt, in organischen Lösungsmitteln zu untersuchen.

Eine sensibilisierte verzögerte Fluoreszenz Reaktion kann mit den folgenden Gleichungen beschrieben werden:



Ein Magnetfeld kann die 4. Gleichung beeinflussen, da es die Energielevel von Triplet Paaren aufspaltet. Diese Paare können entweder im Singlet, Triplet oder Quintet Zustand sein. Während ohne Magnetfeld alle Zustände verfügbar sind, ist die Anzahl der möglichen Zustände in einem starken Magnetfeld anders.

Es wurden der Einfluss eines Magnetfeldes auf die Lebensdauer und die Intensität in unterschiedlichen Sensibilisator/Annihilator Paaren in unterschiedlichen Lösungsmitteln untersucht. Im ZnTPP und Perylene System wurde eine zusätzliche Emission, welche nicht Teil der normalen verzögerten Fluoreszenz ist, beobachtet. Dieses Signal wurde zeigt eine Viskositätsabhängigkeit und wurde weiter analysiert.

Table of Content

1	Introduction.....	1
2	Theory.....	2
2.1	E-Type	2
2.2	P-Type	2
2.3	Radical Recombination	3
2.4	Sensitized Delayed Fluorescence	3
2.4.1	Lifetime.....	7
3	Experiment and Apparatus.....	8
3.1	Chemicals.....	8
3.2	Viscosity	9
3.3	Laser.....	11
3.4	UV-VIS Spectra	14
3.5	Anthracene Measurements.....	14
3.6	Sensitized Measurements	15
3.6.1	Concentration Range.....	18
3.6.2	Spectra.....	20
3.6.3	Lifetime.....	22
4	Results and Discussion	28
4.1	Results Anthracene.....	28
4.2	Results Sensitized Measurements.....	30
4.2.1	ZnTPP and Perylene.....	30
4.2.2	Viscosity Dependence	34

4.2.3	PdTPP and Perylene	41
4.2.4	SnTPP and Perylene.....	42
4.2.5	Comparison different Sensitizer.....	43
4.2.6	Conclusion	43
5	pH-dependent Transient Triplet Absorption.....	45
5.1	Measurement	45
5.2	Results.....	46
5.2.1	Eosin & Cysteine	46
5.2.2	Eosin & Tryptophan.....	49
5.2.3	Erythrosine & Cysteine.....	53
5.2.4	Erythrosine & Tryptophan.....	55
6	Appendix.....	58
6.1	Index of Figures	58
6.2	Index of Tables.....	60
6.3	Index of Equations	60
6.4	Bibliography.....	61

1 Introduction

The motivation for this thesis is the analysis of the influence of an external magnetic field on p-type delayed fluorescence in organic solvents, because this has not been analyzed in detail beforehand. Delayed fluorescence is a well-known process since the 70's but research has mostly been conducted in the solid phase including magnetic field effects. Recently, sensitized delayed fluorescence systems have reappeared titled as "up conversion" in the field of photovoltaics. With this technique it is possible emit light at a higher energy than it is absorbed.

In this work, a sensitized delayed fluorescence system is used in different solvents to analyze the magnetic field effect on it.

In 2 Theory the different types of delayed fluorescence are introduced and sensitized delayed fluorescence is discussed in greater detail.

First during 3 Experiment and Apparatus the used chemicals are listed. Subsequently the applied apparatus and the configuration of these are described. Afterwards the experimental details for the sensitized measurements are explained.

4 Results and Discussion then analyzes the measured results and discusses the possible resolution from the data.

Lastly 5 pH-dependent Transient Triplet Absorption is an extra chapter that describes how I started my PhD thesis and got used to the different apparatuses. Quenching measurements with amino acids were performed and are described in this chapter.

2 Theory

Delayed fluorescence is the emittance of light with the same spectral distribution as prompt fluorescence of the corresponding species, but with a much longer lifetime. Three types exist: E-type, P-type, and radical recombination.

2.1 E-Type

E-type delayed fluorescence happens if the energy difference between the first excited singlet state and the triplet state is smaller than the energy achieved by thermal activation. In this case, triplet states can transform to singlet states via thermal activation. This is depicted in Figure 1.

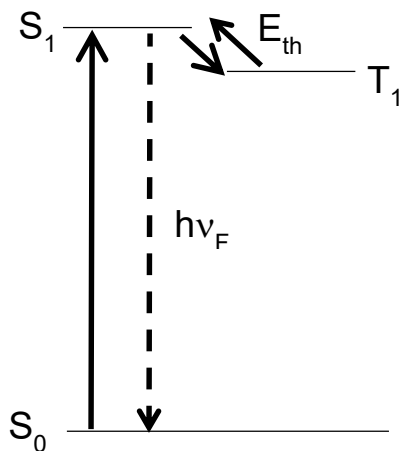


Figure 1 E-Type Energy Schematic

2.2 P-Type

For P-type, delayed fluorescence to occur the energy level of the first excited singlet state has to be about twice the energy of the first excited triplet state. If that is the case, then two triplets can perform a triplet triplet annihilation (TTA) reaction, as can be seen in Figure 2.

There two triplets meet each other and form a triplet triplet encounter pair. Then one triplet molecule transfers its energy to the other. As the energy level of the acceptor triplet is around that of the first excited singlet state it can progress to this state, whereas the donor triplet falls back to the ground state after the exchange.

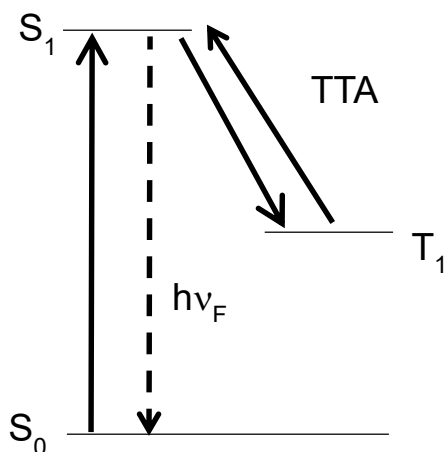


Figure 2 P-Type Energy Schematic

2.3 Radical Recombination

This is the only type of delayed fluorescence that is not dependent on the triplet state but instead requires radical ions. If radical ions recombine with either electrons or radical ions of opposite charges, the first excited singlet state can be populated, from where delayed fluorescence is then emitted.



2.4 Sensitized Delayed Fluorescence

In the system used in this, work (P-type) the delayed fluorescence is originated from the annihilation of two triplet molecules (TTA). As the triplet state of most fluorophores cannot be reached directly by optical excitation (followed by inter system crossing (ISC)) a so

called triplet sensitizer (zinc-meso-tetraphenylporphyrin (ZnTPP)) is applied. The sensitized delayed fluorescence reaction can be summarized by the following equations [1]:

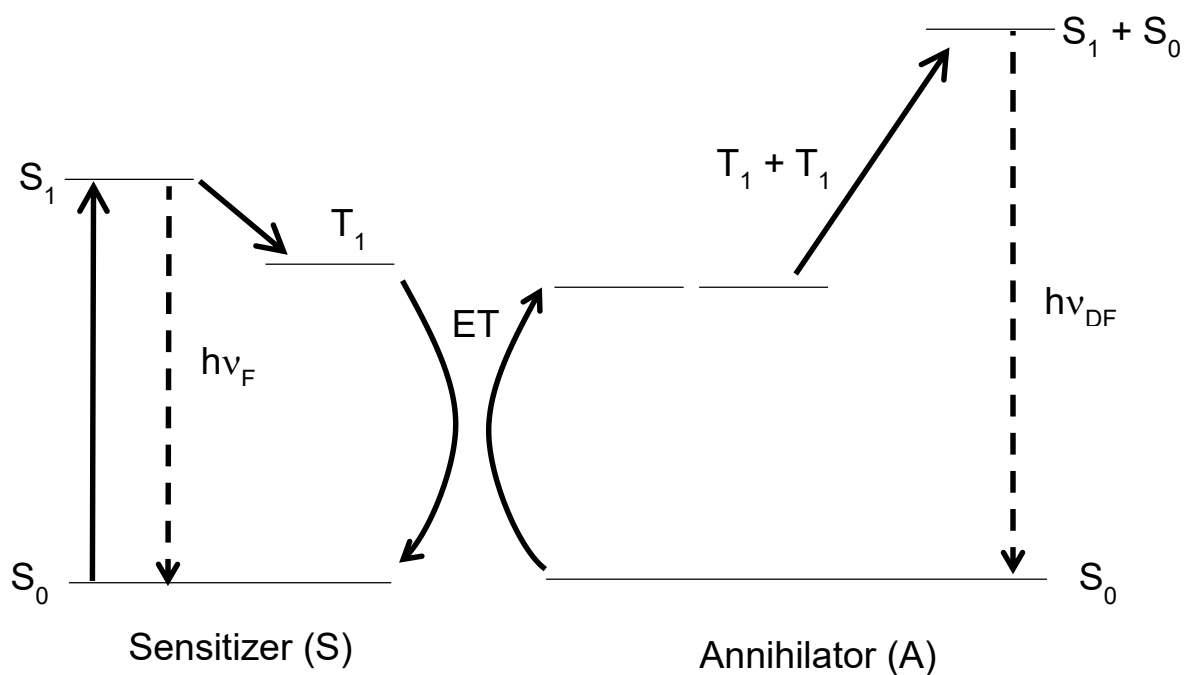
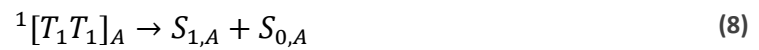


Figure 3 Sensitized Delayed Fluorescence

In equation (4) the sensitizer gets excited, while the annihilator stays in the ground state. Afterwards inter-system crossing occurs (5). If these sensitizer triplets meet an annihilator ground state electron an energy transfer (ET in Figure 3) takes place (6). This can only happen if the triplet energy level of the sensitizer is only slightly larger than the one of the annihilator. With this, annihilator triplets have been generated without exciting the annihilator. For the next step (7) two of these newly generated annihilator triplets have to meet. If that is the case, they form a triplet encounter pair, which can be in a singlet, triplet or quintet state. Only the encounter pairs that are in the singlet state (8) are able to perform a triplet triplet annihilation (TTA) reaction, which generates a singlet in the excited state and a singlet in the ground state. Another requirement for the TTA is that the excited state must have roughly twice the energy of the triplet state. Finally, the annihilator electron that achieved the first excited singlet state can relax to the ground state while emitting light (9).

The delay of this reaction can be explained by the additional time needed before the electrons return to the ground state. In contrast to the prompt fluorescence where the excited S_1 state emits directly, the delayed fluorescence needs a triplet pair as precursor. This pair can annihilate, forming one S_1 and one S_0 state, respectively. The formed S_1 state can emit in contrast to the triplet state. In both cases, the spectral distribution of emission should be the same. As the formation of triplet pairs is essential, the temperature and the viscosity of the solvent also influence the delayed fluorescence. These influences stem from the fact that both properties affect the movement speed of the particles in the solvent. With a higher movement speed, the chance for a collision with another particle in a certain period is increased and this is necessary for the ET and the TTA.

A magnetic field can change the rate of equation (7), as it splits the energy levels of triplet pairs (one singlet, three triplet, and five quintet states). Whereas at zero magnetic field all states are energetically degenerate, with increasing field Zeeman splitting occurs. Between the states a certain amount of mixing exists, which gives a partial singlet character to other states. This is reduced in a high magnetic field resulting in a lower intensity of the delayed fluorescence. [2]

In the solid state, this phenomenon has already been discussed [3]. A triplet pair has nine different states in which it can be. From these the triplet states are the only ones that have an

odd parity under the interchange of two particles. This is the case for all field values. The Hamiltonian and the singlet and quintet states are even and as such, the Hamiltonian can mix the singlet with the quintet states. This means that a quintet state can achieve partial singlet character, and with this TTA is possible. The mixing is dependent on the magnetic field strength and the orientation of the magnetic field with respect to the crystal. If the magnetic field is in one of the resonance directions then no mixing can take place. In case of an off resonance direction, though, it is possible.

In a zero field situation two, in low field all five and in high field only one quintet state(s) can mix. This means that the intensity in a solid state, in case of a magnetic field applied in an off-resonance direction, first increases with increasing magnetic field strength and then starts decreasing.

The splitting of the energy levels of triplet pairs in solvents has been calculated in the literature:

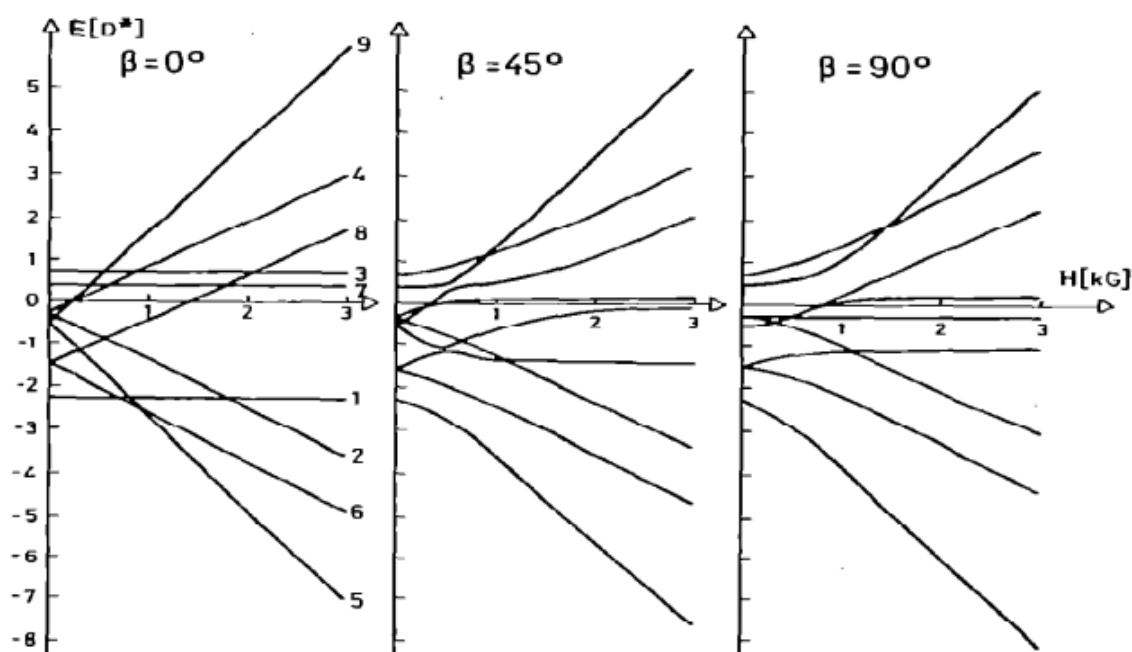


Figure 4 Magnetic field dependence of the energy of triplet pairs for different orientations β of the magnetic field with respect to the direction perpendicular to the molecular plane for $J_Q = 1.24D^1$

¹ Figure taken from (64)

2.4.1 Lifetime

The general assumption for the lifetime of delayed fluorescence is that it is half the lifetime of the triplet state. This is only accurate for a one-molecule system. In case of a sensitized system with different sensitizer and annihilator the lifetime can be calculated by the following formula [1]

$$\tau_{DF} = \frac{\tau_A^0 \tau_S}{\tau_A^0 + \tau_S} \quad (10)$$

As can be seen if $\tau_A^0 = \tau_S$ then the delayed fluorescence lifetime is half of the triplet lifetime.

3 Experiment and Apparatus

In this section, all used chemicals are listed and the different experimental setups that are used are introduced. Furthermore, the performed experiments are explained in detail.

3.1 Chemicals

Name	Company	CAS Nr.
benzene	Fluka puriss p.a. >99,5%	71-43-2
1-octanol	Fluka purum ~98%	111-87-5
paraffin oil	Fluka for IR spectroscopy	8012-95-1
chloroform	Roth >99%, p.a.	67-66-3
cyclohexane	Fluka puriss p.a. >99,5%	110-82-7
p-cymene	Aldrich 99%	99-87-6
heptane	Roth >95% HPLC	142-82-5
mesitylene	Sigma-Aldrich 98%	108-67-8
propyl acetate	Aldrich 99%	109-60-4
toluene	Fluka purum >99%	108-88-3
dimethyl form amide	Roth Rotipuran 99,8%	68-12-2
5,10,15,20-tetraphenyl-21H,23H-porphyrin	Sigma Aldrich	917-23-7
zinc chloride	Aldrich >98%	7646-85-7
palladium chloride	Aldrich Reagent Plus 99%	7647-10-1
tin chloride	Aldrich 98%	7772-99-8
magnesium chloride	Roth >98,5% water free	7786-30-3
cadmium chloride	Aldrich 99.99%	10108-64-2
zinc-meso-tetraphenylporphyrin (ZnTPP)		
palladium-meso-tetraphenylporphyrin (PdTPP)		
tin-meso-tetraphenylporphyrin (SnTPP)		
magnesium-meso-tetraphenylporphyrin (MgTPP)		
perylene	Aldrich >99,5% sublimed	198-55-0

anthracene	Fluka >99% suitable for scintillation	120-12-7
anthracene	Gold Label 99,9%	120-12-7

Table 1 Chemicals

ZnTPP has been synthesized from 5,10,15,20-tetraphenyl-21H,23H-porphine and zinc chloride according to [4]. The other tetraphenylporphyrin compounds have been synthesized using the same method with the corresponding metal salts. Perylene was delivered by Sigma-Aldrich and has been sublimed. Benzene has been distilled and dried (molecular sieve 4Å) before use.

3.2 Viscosity

For the viscosity measurements, an Ubbelohde viscometer was used. These measurements were necessary to further analyze a behavior, which could be observed during the sensitized delayed fluorescence measurements, because a viscosity dependence of this behavior was suspected. This will be explained in detail in chapter 4.2.2.

The lower glass block with the Water In and Water Out marks is the connection to the water bath and is not connected to the interior, which was filled with water and stirred, so that the upper parts are also tempered. The grey lines at the top of the leftmost column are the marks for stopping the time.

The viscometer was filled with approximately 20ml of the solvent mixture. Different mixtures were used to achieve different viscosity values. The composition of these mixtures is described in chapter 3.6. The minimum volume needed for the measurement is 15ml. After waiting for about 20 minutes, to allow the temperature to adjust, the measurements were started, by measuring the time the fluid needs to fall from the upper marker to the lower one. The resulting time was multiplied by an instrument constant to get the kinematic viscosity; multiplying the latter with the measured density results in the dynamic viscosity. The instrument constant was taken from [4] and checked by measuring solvents with known viscosity at different temperatures. At higher temperatures, the same constant can still be used, because the difference from the expansion of the capillary at higher temperatures influences the resulting viscosity only on a small scale that is still within the measurement error.

3 EXPERIMENT AND APPARATUS - 3.2 VISCOSITY

The viscosity measurements are discussed in chapter 3.6.

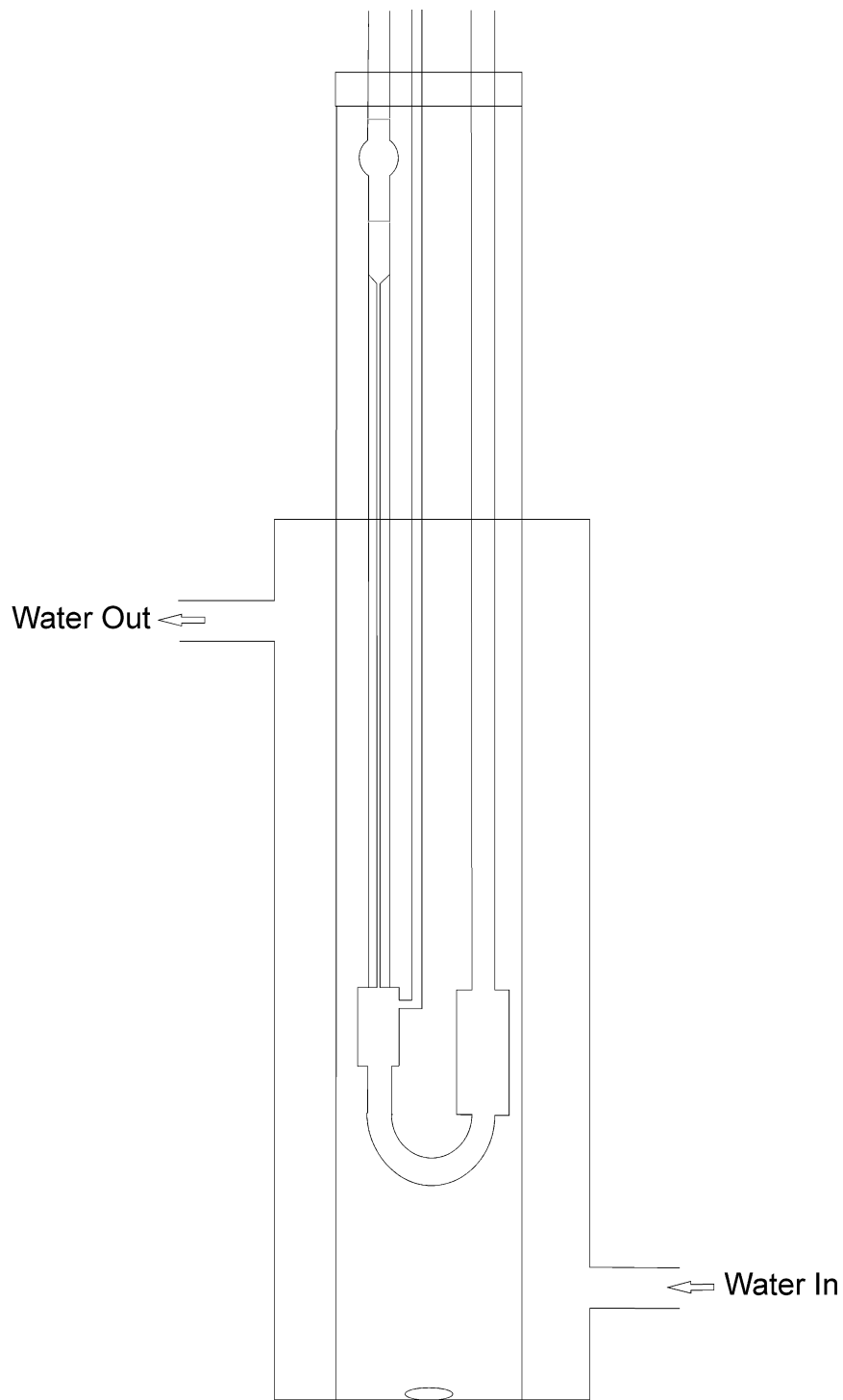


Figure 5 Ubbelohde Viscometer

3.3 Laser

As excitation source a dye laser (Coumarin 153, $\lambda=520-600\text{nm}$, $\lambda_{\text{peak}}=540\text{nm}$) pumped by a XeCl excimer laser ($\lambda_{\text{max}}=308\text{nm}$, pulse width 10ns) was used. The cuvette containing the sample was placed inside an electro-magnet (Buckley Systems LTD). The field strength was measured with a Gauss-meter (Bell 9200) near the sample. The delayed fluorescence signal was detected perpendicularly to the excitation beam, which enters the cuvette from the bottom, due to geometrical limitations of the magnet. For the detection, a photomultiplier tube (PMT) was used with a monochromator installed in the emission path (473nm for the perylene fluorescence). The signal from the PMT was recorded by a digital storage oscilloscope (LeCroy 9350C). A photodiode, which detects a small part of the XeCl laser emission, was used to send a trigger signal to the oscilloscope. Following this trigger signal the oscilloscope started recording for a specific amount of time, depending on the setting of the time resolution.

A second PMT was used to detect the weak ZnTPP fluorescence. A long pass filter with a 50% cutoff at 590nm was installed in the beam path to remove the perylene fluorescence from this channel. Only ZnTPP emits at wavelengths higher than 590nm (see Figure 12). This detection channel was added to reduce the influence of the varying excitation intensity of each single laser shot. ZnTPP fluorescence is directly proportional to the excitation intensity while the delayed fluorescence has a quadratic dependency. By checking the varying ZnTPP fluorescence intensity, these fluctuations can be accounted for.

This setup allows time dependent measurements of the delayed fluorescence signal at a single wavelength with ns resolution.

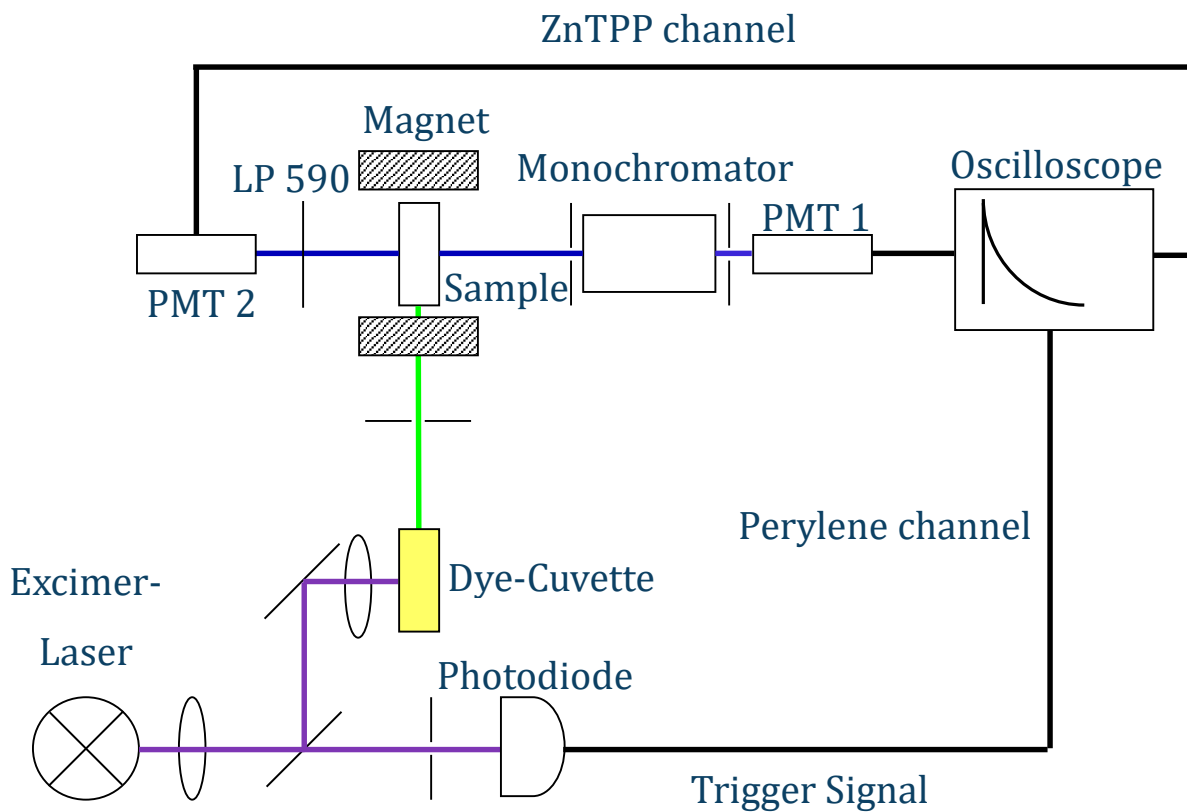


Figure 6 Laser Setup 1

The following Figure 7 shows the cuvette from the side to better demonstrate how the laser enters the sample:

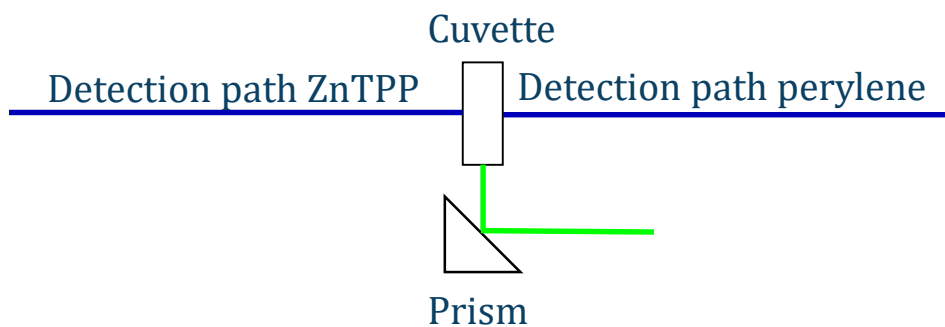


Figure 7 Side View of Cuvette

For measuring the absorption the following modification with a 473nm laser (dragon lasers, MLL-FN-473-50mW) has been used:

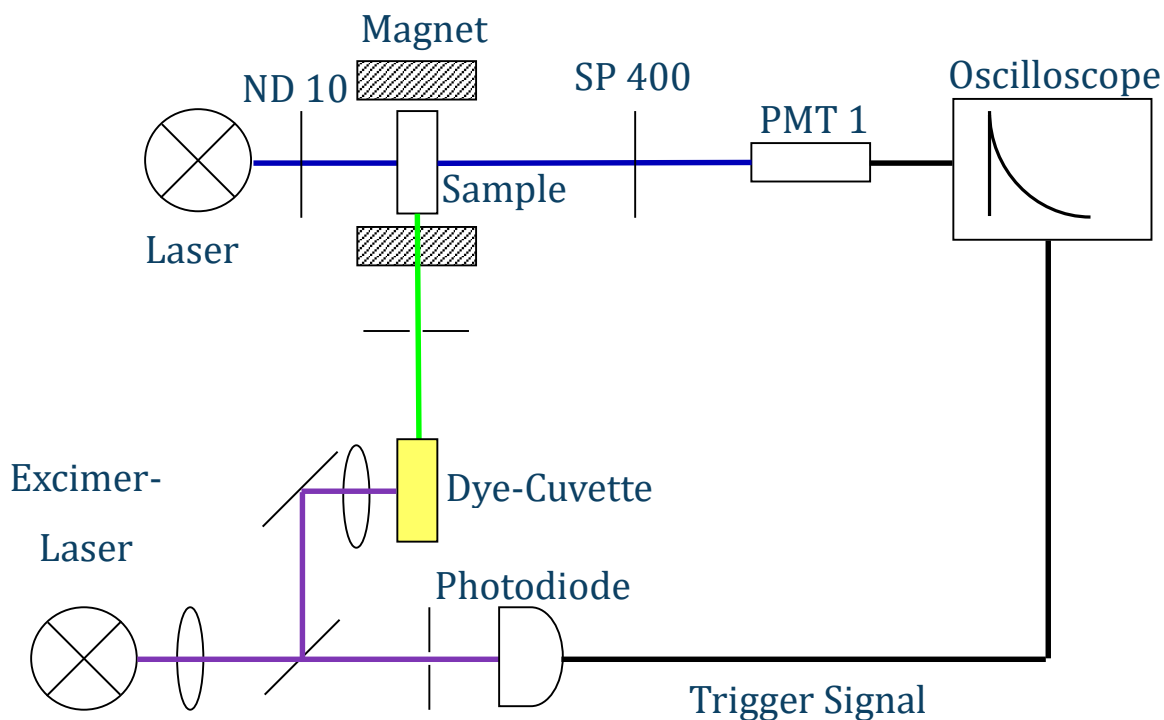


Figure 8 Laser Setup 2

The difference is that in Figure 6, the light emitted from the sample is picked up by a light guide directly next to the sample and is guided to the monochromator, whereas in Figure 8, the light from the laser goes through air after the sample until it is picked up by a light guide and guided to the PMT. As fluorescence signals scatter fast and the observing light is a focused laser light, Laser Setup 2 ensures that no fluorescence signal is detected. This was tested by irradiating the mixture without the observing laser and no signal could be detected.

The used filters are a long pass 590 (LP 590) and a short pass 400 (SP 400). The number denotes the wavelength at which 50% of the light is absorbed. While long pass filters cut off lower wavelengths (i.e. in case of the LP 590 wavelengths below 590 are filtered out), short pass filters cut off higher wavelengths. Furthermore, a neutral density filter (ND 10) has been used to decrease the strength of the observing laser. This filter has an absorption of 1.0 across the visible region of the spectrum.

3.4 UV-VIS Spectra

For the measurements of the UV-VIS absorption spectra, a Shimadzu UV-3101PC UV-VIS-NIR Scanning Spectrophotometer was used.

3.5 Anthracene Measurements

To all measurements applies that the system was poled in a way that a negative voltage was measured. This means that a more negative value corresponds to a higher intensity. For example -0.6V is a higher intensity signal than -0.4V.

The first measurements to analyze the behavior of delayed fluorescence were done with anthracene according to [5]. First measurements were done in DMF without magnetic field with concentrations of $1.4 \times 10^{-4} \text{M}$, $3.5 \times 10^{-4} \text{M}$ and $5 \times 10^{-4} \text{M}$ of anthracene. Magnetic field dependent measurement were only performed with a concentration of $5 \times 10^{-4} \text{M}$ as this gave the best signal.

The following magnetic field dependence measurements were done. For all these measurements excitation was at 308nm and detection of emission at 420nm and Laser Setup 1 without the ZnTPP channel was used.

1st: Measurement from 500G to 5500G

2nd: Measurement from 0G to 3500G, measurement of blank for scatter peak first

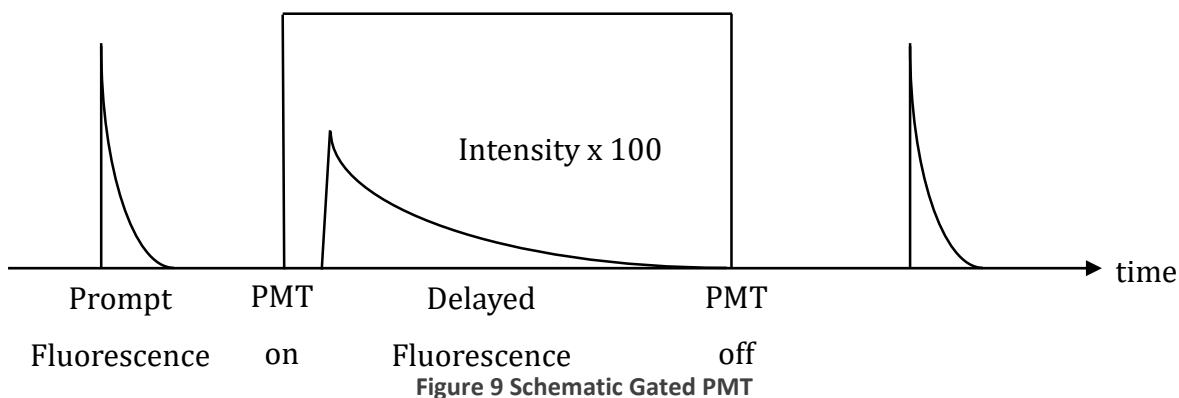
3rd: two measurements from 0G to 3500G, poles have been changed between measurements

4th: two measurements from 3500G downwards to 0G, poles have been changed between measurements

5th: batch solution has been prepared and for each measurement a new sample from the batch has been taken. Only approximately 10 laser shots, which were then averaged, were measured for each measured point to decrease the exposure to the exciting laser as much as possible. Measurement from 0 to 4000G

6th: changed to anthracene gold label 99.9%, batch solution has been prepared and for each measurement, a new sample from the batch has been taken. Once again, only approximately 10 laser shots were averaged for each measured point. Measurement from 0 to 7000G.

For future measurements, a gated PMT setup was devised. This was done in order to prevent an overload of the PMT from the prompt fluorescence, which is approximately 100 times stronger than the delayed fluorescence. If the PMT is overloaded, it takes some time before it can react again and the signals recorded during this time are not correct. A gated PMT means that the active and inactive phase of the PMT is controlled, see Figure 9 Schematic Gated PMT. During the inactive time, the PMT will not receive any input signals. During that time, the prompt fluorescence arrives. A short timescale after the PMT is activated and can measure signals. During that period, the delayed fluorescence arrives and is measured by the PMT. The idea is to set the time from the laser excitation to the activation of the PMT to such a length that nothing from the prompt but everything from the delayed fluorescence is detected. The PMT then needs to become inactive again before the next laser pulse arrives.



3.6 Sensitized Measurements

Also for all sensitized measurements applies that a more negative voltage correlates to a higher intensity. For example -0.1V is a lower intensity signal than -0.5V .

For the sensitized measurements, perylene has always been chosen as annihilator while for the sensitizer the following three porphyrins were used:

- a) ZnTPP
- b) SnTPP
- c) PdTPP

CdTPP and MnTPP have also been synthesized but these two did not show any delayed fluorescence with perylene. Most experiments, especially in the initial stage, have been performed with ZnTPP. These experiments have been used to understand the system, optimize the setup and the procedure. Afterwards other sensitizers have been used to see how much influence a change of the metal center has on the delayed fluorescence.

Measurements have been performed in the following solvents, although not every composition has been measured in each solvent:

- a) Acetonitrile
- b) Acetone
- c) Benzene
- d) Mixtures of benzene and paraffin oil
- e) Chloroform
- f) Cyclohexylbenzene
- g) Cymene
- h) Mesitylene
- i) Octanol
- j) Paraffin oil
- k) Propyl acetate
- l) Toluene

Mixtures of benzene and paraffin oil have been prepared to observe the dependence on the viscosity. The following viscosities have been achieved:

3 EXPERIMENT AND APPARATUS - 3.6 SENSITIZED MEASUREMENTS

Viscosity [cP]	Mole fraction paraffin oil	Mole fraction benzene
0.6	0	1.000
2.0	0.425	0.575
3.8	0.584	0.416
7.1	0.707	0.293
19.8	0.844	0.156
25.3	0.871	0.129
29.6	0.889	0.111
41.6	0.923	0.077
95.0	1.000	0

Table 2 Viscosity mixture composition (benzene/paraffin oil)

The mole fractions for these mixtures have first been calculated according to the following formulas [6]:

$$\eta = \nu * \rho \quad (11)$$

$$\nu_{mix} = e^{e^{\frac{VBN_{mix}-10.975}{14.534}}} - 0.8 \quad (12)$$

$$VBN_{mix} = \sum_{i=0}^n w_i * VBN_i \quad (13)$$

$$VBN_i = 14.534 * \ln(\ln(\nu_i + 0.8)) + 10.975 \quad (14)$$

η = dynamic viscosity in cP

ν = kinematic viscosity in cSt

ρ = density in g/cm³

w = mass fraction

VBN = viscosity blending number

Afterwards the viscosity of the mixture has been measured using an Ubbelohde viscometer. Viscosity measurements have been performed at room temperature.

For the laser measurement, the sensitizer and annihilator have been dissolved in the corresponding solvent. Afterwards Argon 5.0 has been bubbled through the solution in an argon atmosphere, which was saturated with solvent vapor, for 30 minutes in order to remove the oxygen. To achieve the saturation of the gas a washing bottle has been used (see Figure 10), which was filled with solvent, where the gas is guided through. This step is important for volatile solvents, because the gas can easily vaporize these solvent molecules. If the gas has not been saturated beforehand, the solvent molecules will be taken from the probe, which means that the amount of solvent decreases, the longer the sample is bubbled. Therefore, the concentration is changed. To prevent this effect gas saturation beforehand is important.

Measurements were performed both from low field to high field and vice versa to make sure there is no influence on the emission signal.

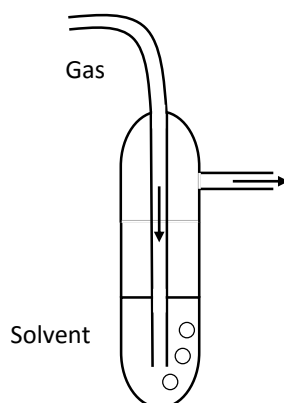


Figure 10 Schematic Gas Saturation

3.6.1 Concentration Range

In order for a sensitized system to show delayed fluorescence with an acceptable intensity a certain balance of concentrations has to be achieved. During the process, a sensitizer triplet has to meet with an annihilator ground state for the energy transfer to take place. If the concentration of the sensitizer is too high, the chance to meet with an annihilator, and in consequence the intensity, goes down. Afterwards two annihilator molecules have to meet for the triplet triplet annihilation reaction. Once again if the concentration of the sensitizer is too high the intensity decreases. In contrast, the concentration of the sensitizer regulates how

many molecules can be excited at maximum, so this concentration cannot be too low either. Measurements with varying degrees of concentrations for ZnTPP as sensitizer and perylene as annihilator in benzene were performed and the intensity of the delayed fluorescence signal was observed.

As can be seen in Figure 11 if the concentration of sensitizer is too low ($1 \times 10^{-5} \text{M}$ seen at green and black line) or the concentration of the sensitizer is higher than the concentration of the annihilator (red line) then the intensity is low. If both have the same concentration (pink line), the intensity is higher but not yet at a satisfactory level. If a high concentration of annihilator with a high enough concentration of sensitizer (both blue lines) is used a good intensity can be achieved. The doubling of the annihilator concentration (dark blue in contrast to light blue) only increased the intensity a slightly. As such, it is assumed that this is close to a plateau and a concentration of $5 \times 10^{-4} \text{M}$ for the annihilator and $1 \times 10^{-4} \text{M}$ for the sensitizer was used for the following experiments.

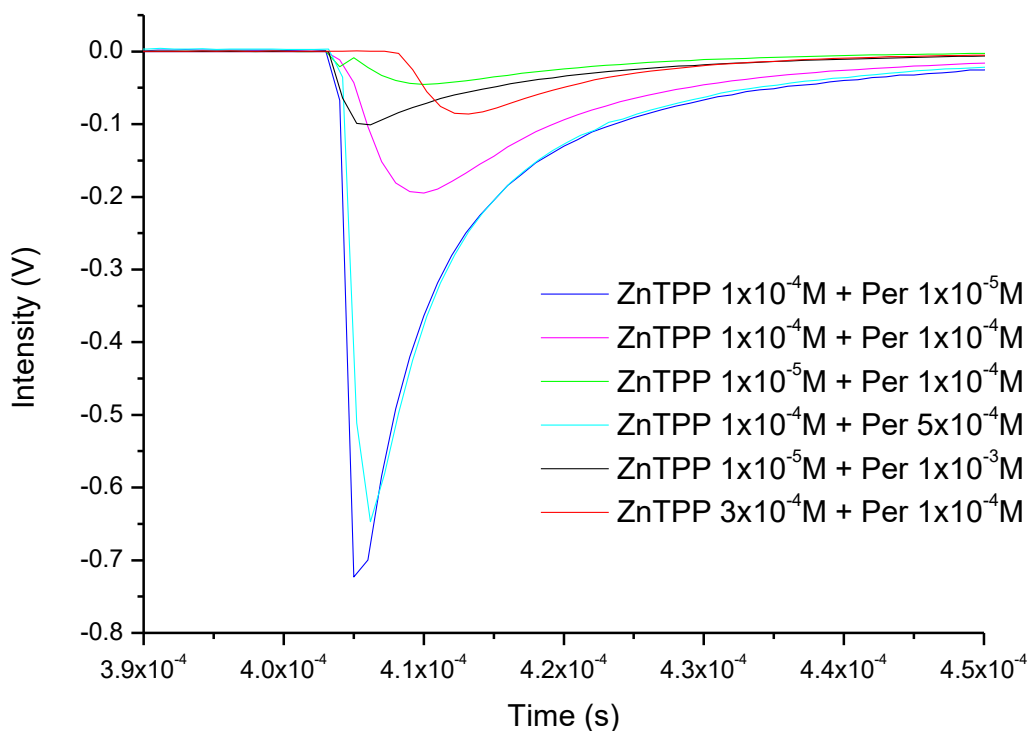


Figure 11 Concentration range measured in benzene

3.6.2 Spectra

In order to set up the experiment corresponding wavelengths had to be chosen. In order to do that absorption and fluorescence spectra of all relevant chemicals are necessary.

The triplet absorption spectrum of the sensitizer in Figure 12 to Figure 14 was measured using transient absorption with the laser setup, while the other absorption and fluorescence spectra have been recorded with Shimadzu UV-VIS spectrophotometer.

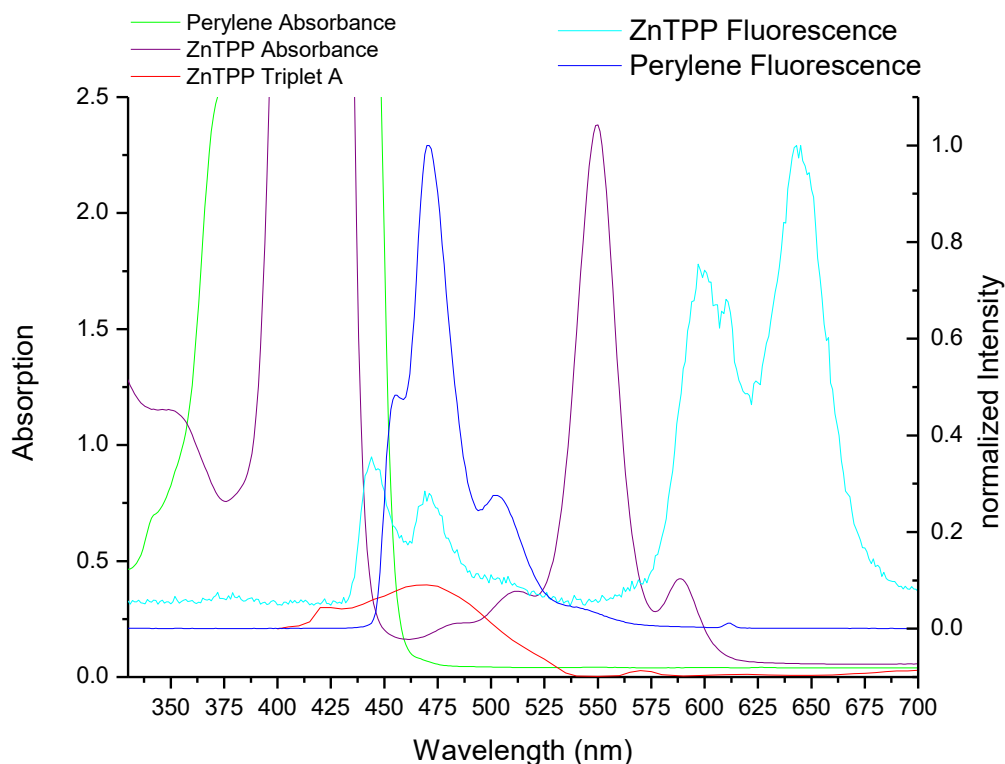


Figure 12 Spectra of ZnTPP and perylene in benzene

3 EXPERIMENT AND APPARATUS - 3.6 SENSITIZED MEASUREMENTS

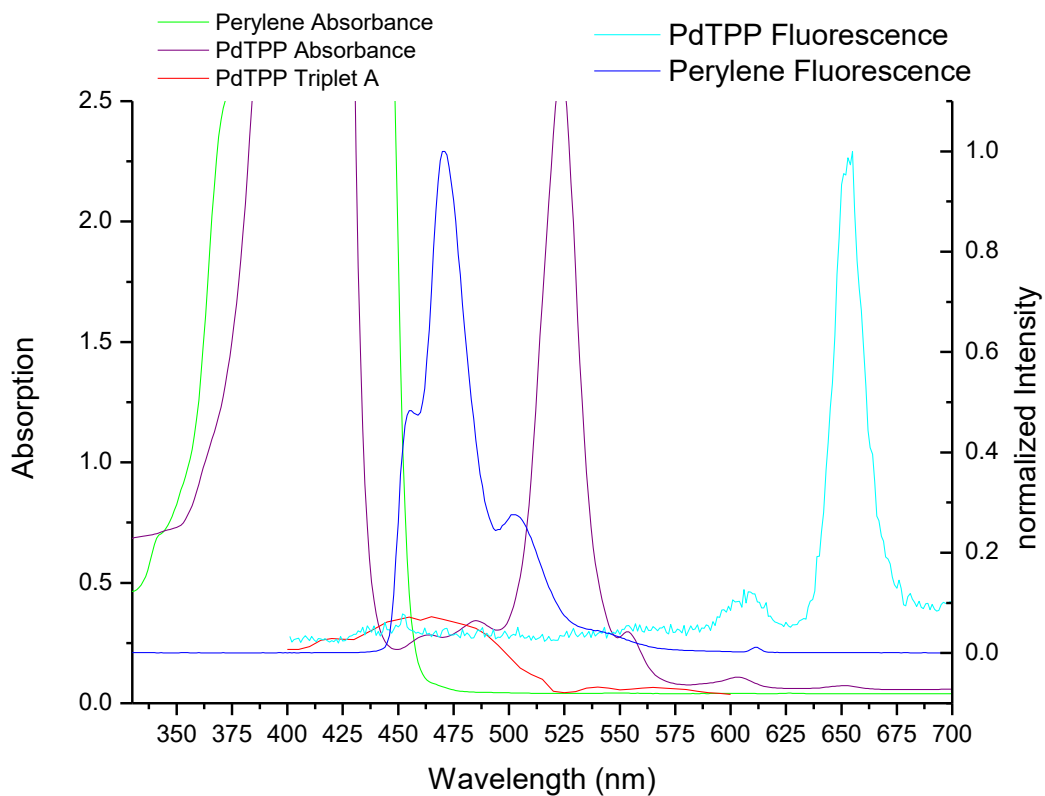


Figure 13 Spectra of PdTPP and perylene in octanol

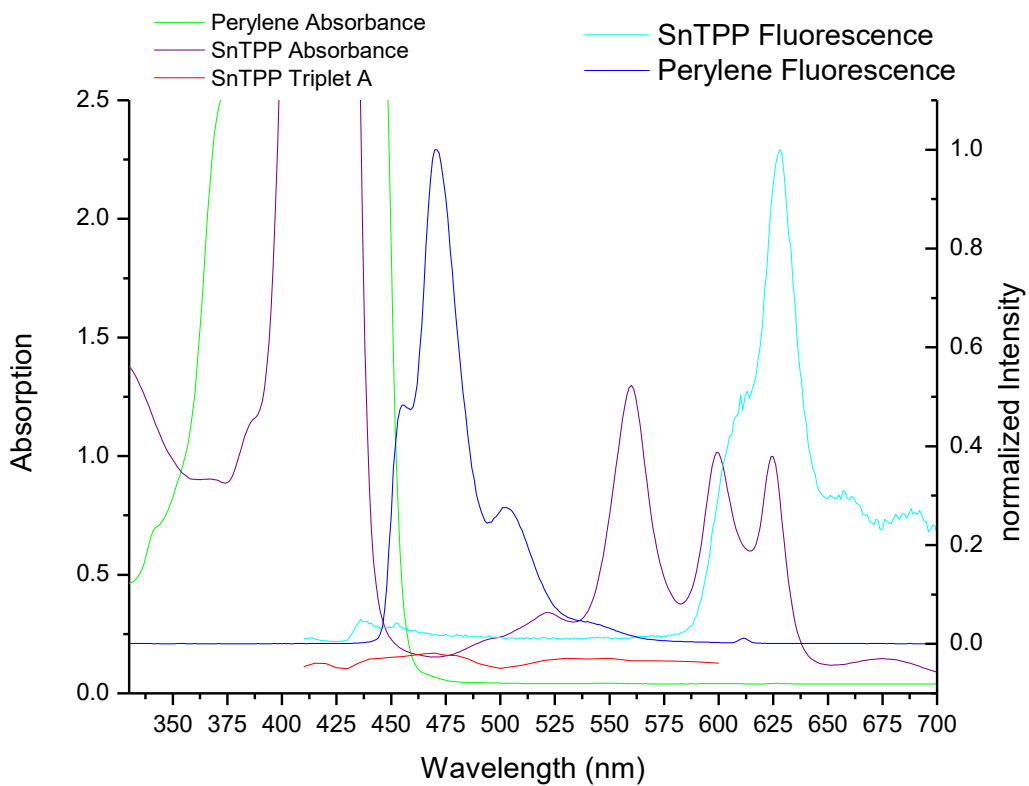


Figure 14 Spectra of SnTPP and perylene in octanol

For the excitation only the sensitizer and not the annihilator should be excited to guarantee that the only way to get S_1 sensitizer molecules is via TTA. As perylene only absorb until approximately 460nm and the different metal TPPs have an absorption band in the 500nm region a coumarin 153 dye laser was chosen for excitation, which emits in the region between 520nm and 600nm with a peak at 540nm. Measurements with only perylene showed no fluorescence signal with this laser. As such, it is assured that no excitation is happening. For the detection, 473nm was chosen, because that is near the maximum of the perylene emission and the TPP fluorescence at this wavelength is so small (20 times less intensity than perylene before normalization) that it can be neglected, and there are lasers available at this wavelength. At 473nm, there is still absorption from the TPP triplet and ground state. This means that the detected emission has already been partially absorbed. For this reason, a transient absorption measurement was performed at this wavelength with a corresponding laser as the observing light. With this information, the original emission data can be calculated.

3.6.3 Lifetime

Lifetime measurements were conducted to see if there is any influence from the magnetic field on the lifetime of the delayed fluorescence emission.

To calculate the lifetime from the data, the originally measured emission spectra have been modified with the data received from transient absorption spectra. Therefore, if at time, t , the measured absorption was 30% that means that only 70% of the intensity of the fluorescence signal was detected. So the measured point in the original emission spectrum at time t was then divided by 0.7. This corrects the value of the data point to the original value that should have been emitted, before part of it was absorbed. This calculation is then done for every data point. The original curve can be seen in Figure 15, while a comparison between the calculated one and the measured one can be seen in Figure 16.

Then the resulting curve (calculated data in Figure 16) was fitted. A fit according to a first order reaction was not applicable, which can be seen by looking at Figure 17. The residuals start to actually get close to the curve at approximately $6 \cdot 10^{-5}$ seconds. At this point in time, the intensity is almost at 0 again. Therefore, for the period where there is actually an emission the fit is off quite a lot.

3 EXPERIMENT AND APPARATUS - 3.6 SENSITIZED MEASUREMENTS

The reason for the bad fit is that two reactions occur simultaneously. The emission of the perylene depends on the triplet state of TPP, which can decay back to the ground state (first order) or perform a triplet triplet annihilation (second order). As such, there is a mixture of first and second order reaction.

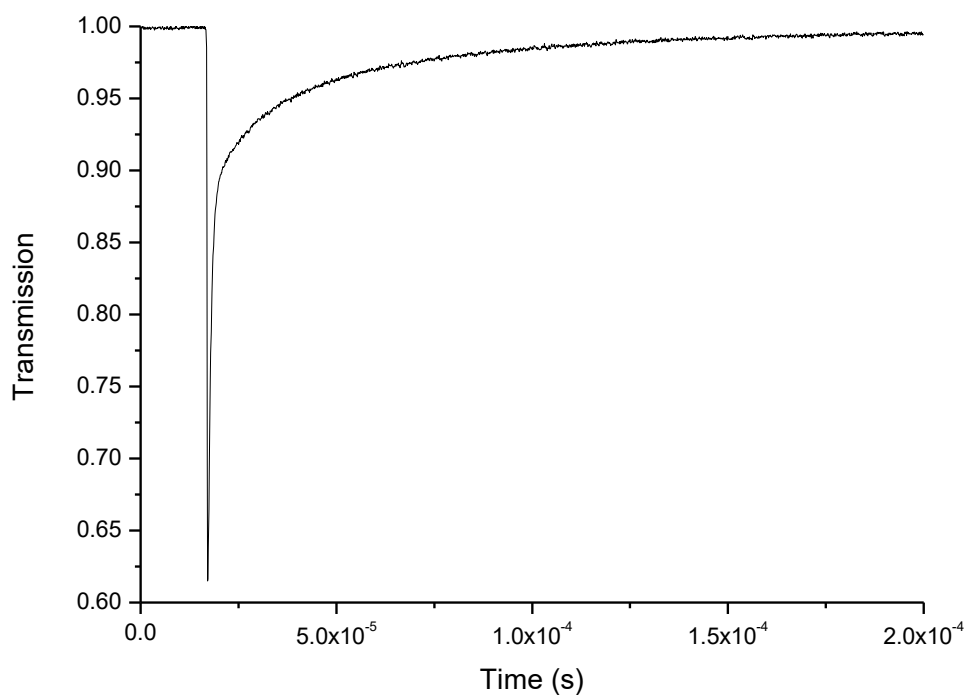


Figure 15 Absorption trace of ZnTPP ($1 \times 10^{-4} \text{M}$) and perylene ($5 \times 10^{-4} \text{M}$) in benzene

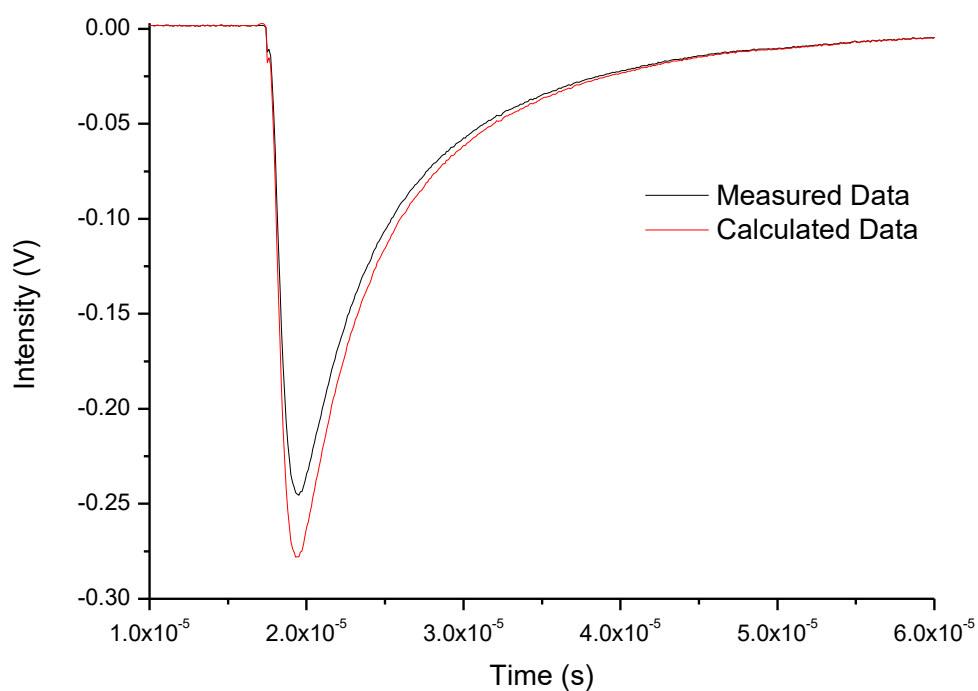


Figure 16 Comparison of measured and calculated decay curve of ZnTPP ($1 \times 10^{-4} \text{M}$) and perylene ($5 \times 10^{-4} \text{M}$) in benzene

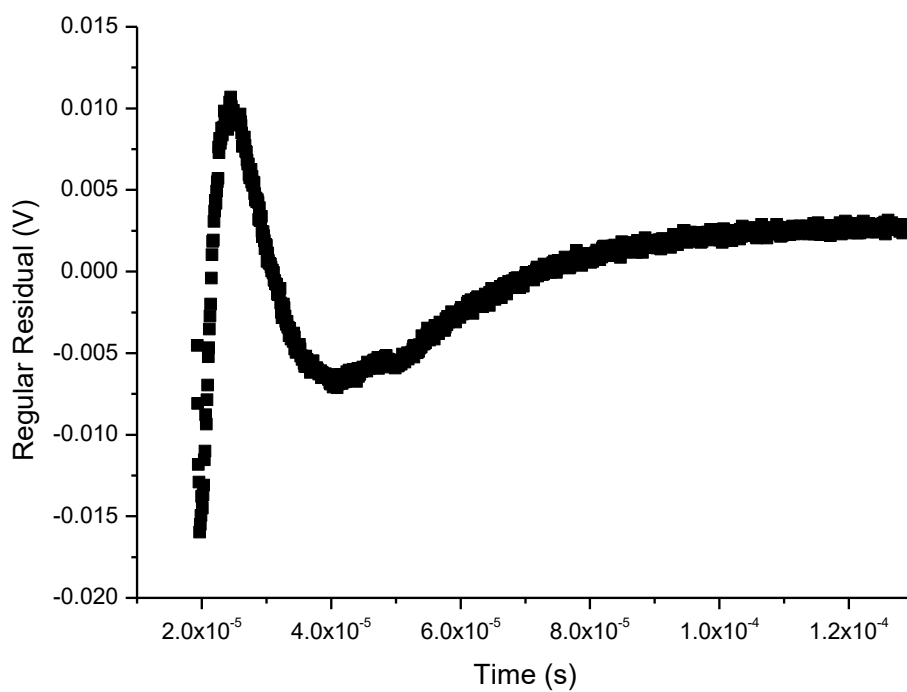


Figure 17 Residuals of First Order Fit

The most accurate formula found in literature to describe this was the following one [7]:

$$I_t = \alpha \left(\frac{[T]_0 e^{-k_1 t}}{1 + (1 - e^{-k_1 t}) \frac{2k_{TTA}}{k_1} [T]_0} \right)^2 \quad (15)$$

I_t = emission intensity at time t

α = experimental parameter

$[T]_0$ = initial triplet concentration at the time of the laser excitation

k_1 = first order rate constant, which includes the first order decay and any impurity quenching process

k_{TTA} = rate constant of the triplet triplet annihilation reaction

The initial triplet concentration was obtained by doing a time correlated transient absorption measurement of ZnTPP. Using the Lambert-Beer formula (16) $[T]_0$ could be calculated, as the extinction coefficient is known from literature.

$$E_\lambda = \varepsilon_\lambda * c * d \quad (16)$$

By using this formula, the fit quality increased significantly. It is still not a good fit but it is satisfactory enough to give an idea about the change of the lifetime with varying magnetic field strength.

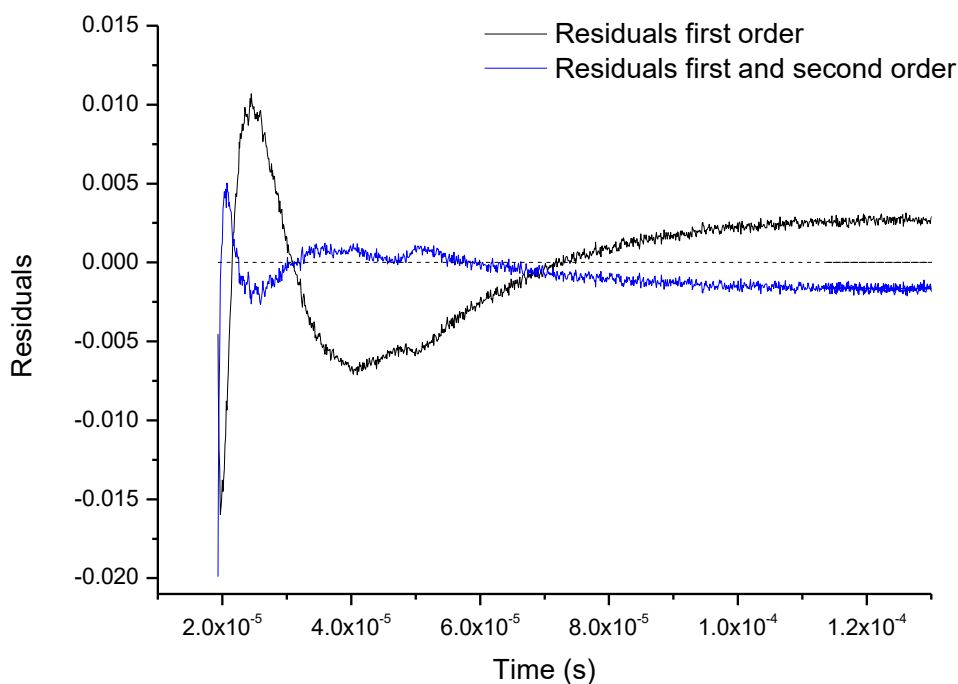


Figure 18 Residuals for both fits

As can be seen in Figure 19, there is only a small change in the lifetime, which does not seem to be influenced by the magnetic field strength. As such, it is assumed that there is no magnetic field dependence on the lifetime of the delayed fluorescence. This is in agreement with the reaction mechanism discussed in 2.4 Sensitized Delayed Fluorescence, as the magnetic field only influences the amount of triplet pairs that can perform triplet triplet annihilation, but does not have any effect on the time the electron stays in the first excited singlet state of the annihilator. As a result no further measurements of the lifetime were performed.

3 EXPERIMENT AND APPARATUS - 3.6 SENSITIZED MEASUREMENTS

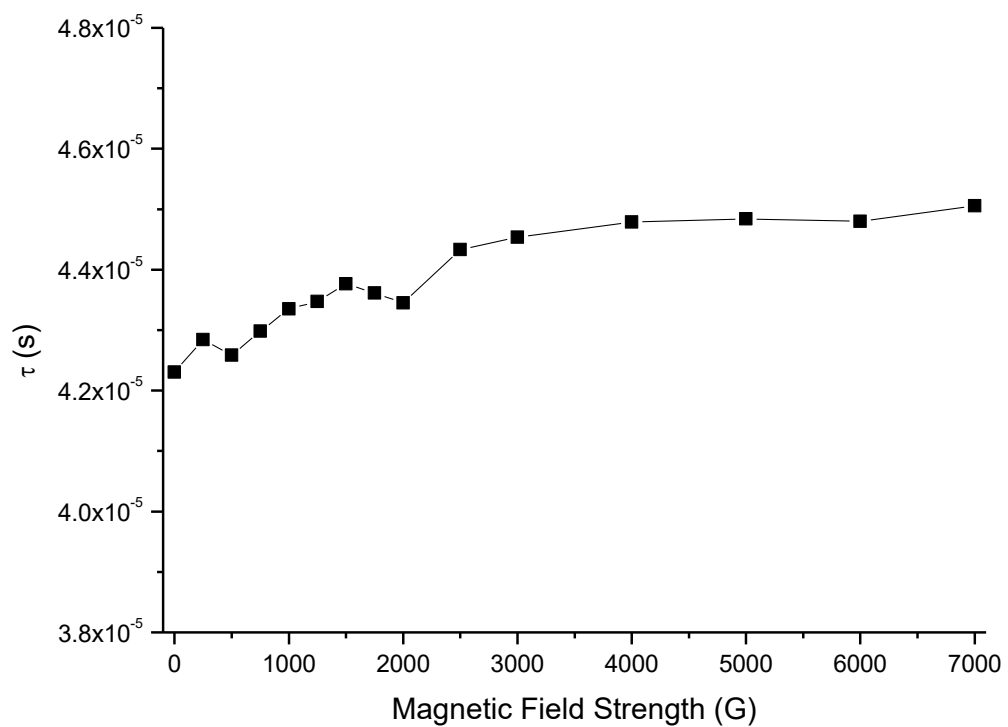


Figure 19 Dependency of Lifetime to magnetic field strength of ZnTPP ($1 \times 10^{-4} \text{M}$) and perylene ($5 \times 10^{-4} \text{M}$) in benzene

4 Results and Discussion

4.1 Results Anthracene

Anthracene measurements were done in DMF with varying concentrations and under different experimental settings. Still the measurements performed on anthracene did not yield any good results, as it is almost impossible to make a meaningful distinction between the prompt and the delayed fluorescence in the spectra. Part of the problem is that the prompt fluorescence overloads the PMT.

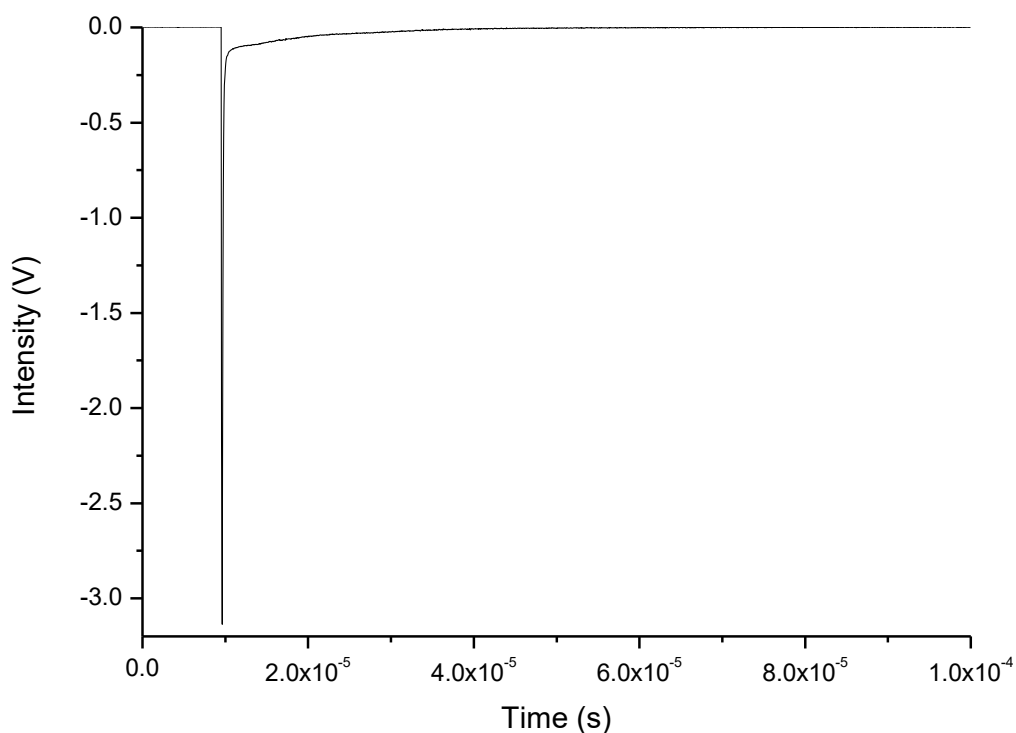


Figure 20 Emission trace of anthracene (5×10^{-4} M) in DMF

As can be seen, first there is a strong increase, which comes from prompt fluorescence. The decline of the decreasing slope becomes at one point much less steep than before and then expected. This derives from the delayed fluorescence, which is overlapped with the prompt one. As such, it is very difficult to separate the two and make a meaningful analysis of the

delayed fluorescence from this data. What can still be derived from that is that a delayed fluorescence exists as otherwise, there would be a steep decline of the peak, and that this delayed fluorescence is magnetic field dependent as can be seen in Figure 21

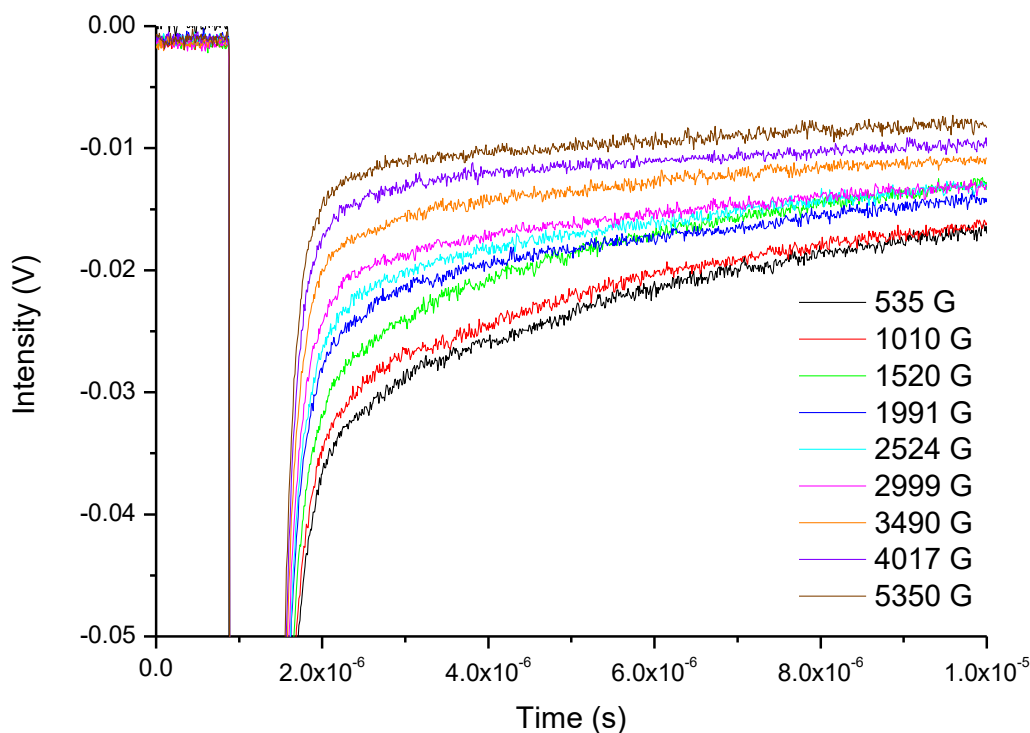


Figure 21 Magnetic field effect anthracene ($5 \times 10^{-4} \text{M}$) in DMF

It can also be noted that anthracene seems to degrade by being exposed to continuing laser shots. For this reason, a batch solution has been created and for each measurement, a new sample from the batch has been taken to get an idea about the magnetic field dependence. To obtain more detailed measurements, in the future, another setup would have to be used. The first measurements [5] in literature by Faulkner were done by using a synchronized rotating disc setup to separate the prompt fluorescence from the delayed one. Another possibility would be to use the gated PMT setup, described in 3.5.

4.2 Results Sensitized Measurements

4.2.1 ZnTPP and Perylene

Measurements have been performed in different solvents. In acetonitrile and propyl acetate, the fluorescence signal was too weak to warrant further measurements. Chloroform seems to decompose during the measurement. For the rest of the solvents measurements have been performed. The following figures display the average maximum intensities obtained at various magnetic fields in different solvents:

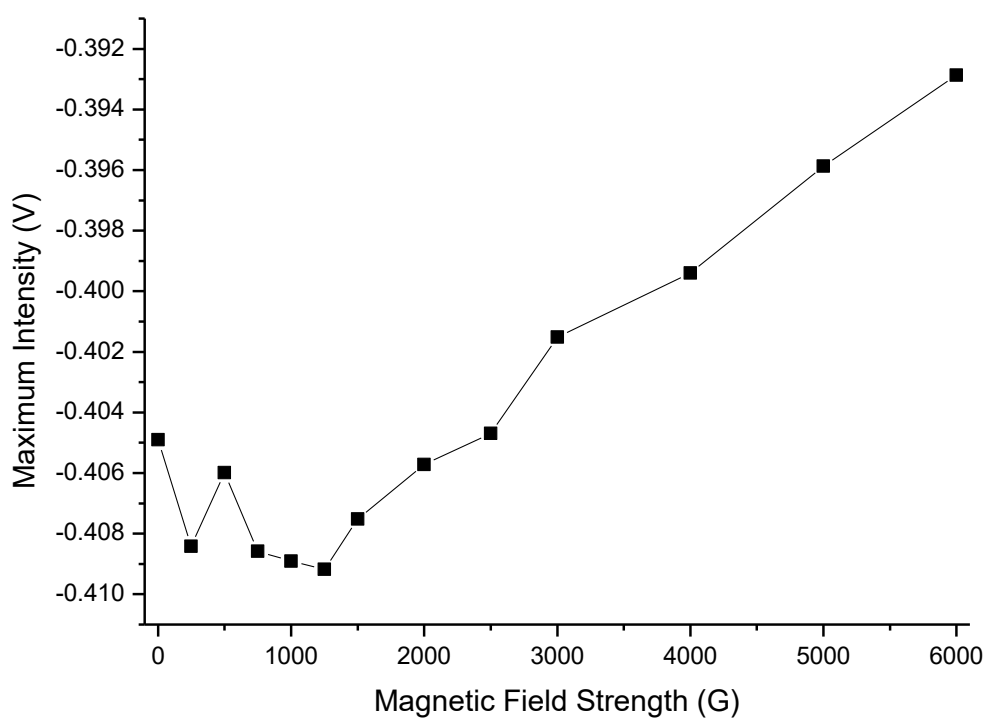


Figure 22 Delayed Fluorescence ZnTPP + perylene in acetone

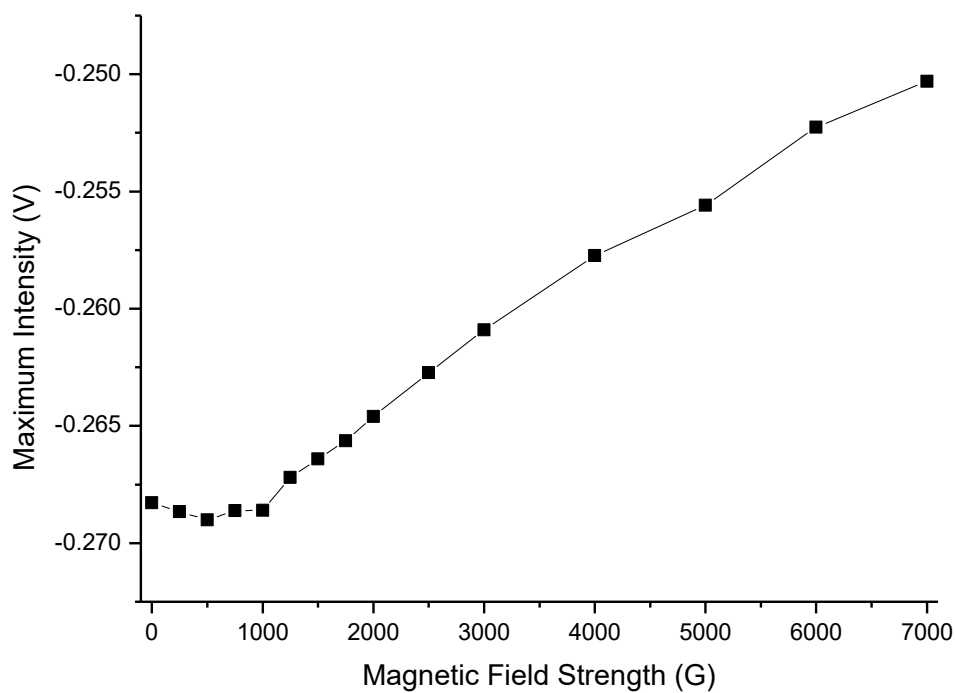


Figure 23 Delayed Fluorescence ZnTPP + perylene in benzene

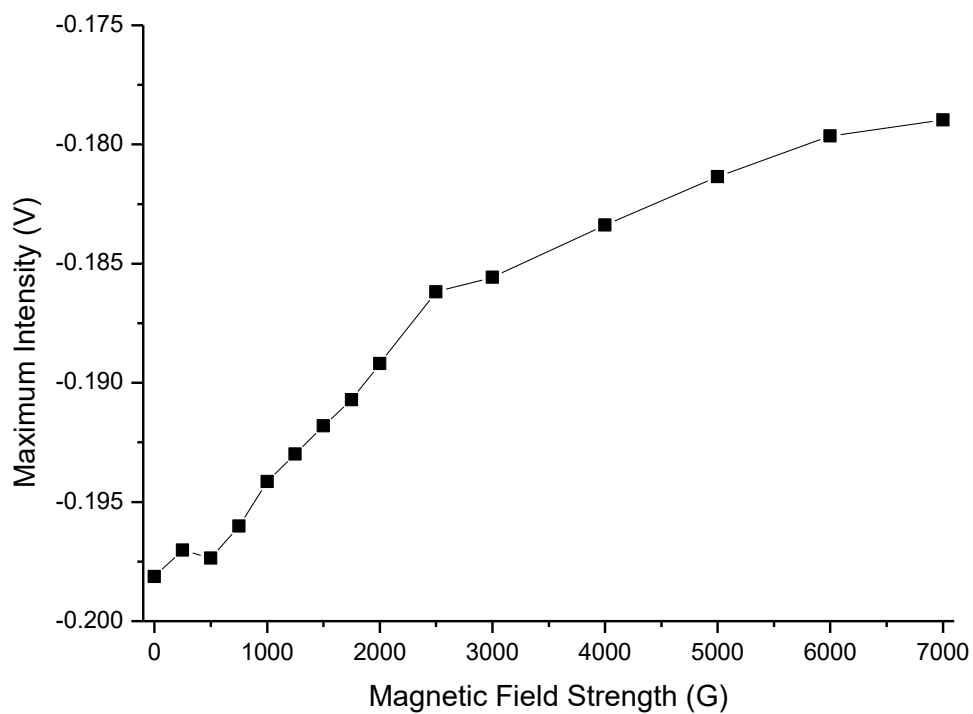


Figure 24 Delayed Fluorescence ZnTPP + perylene in cyclohexylbenzene

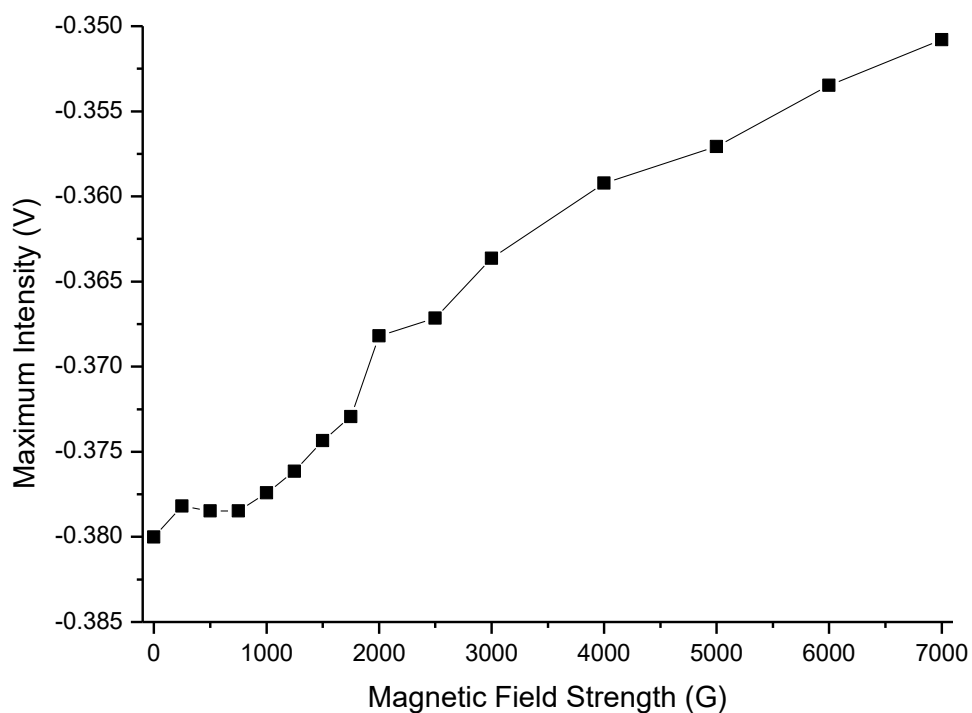


Figure 25 Delayed Fluorescence ZnTPP + perylene in cymene

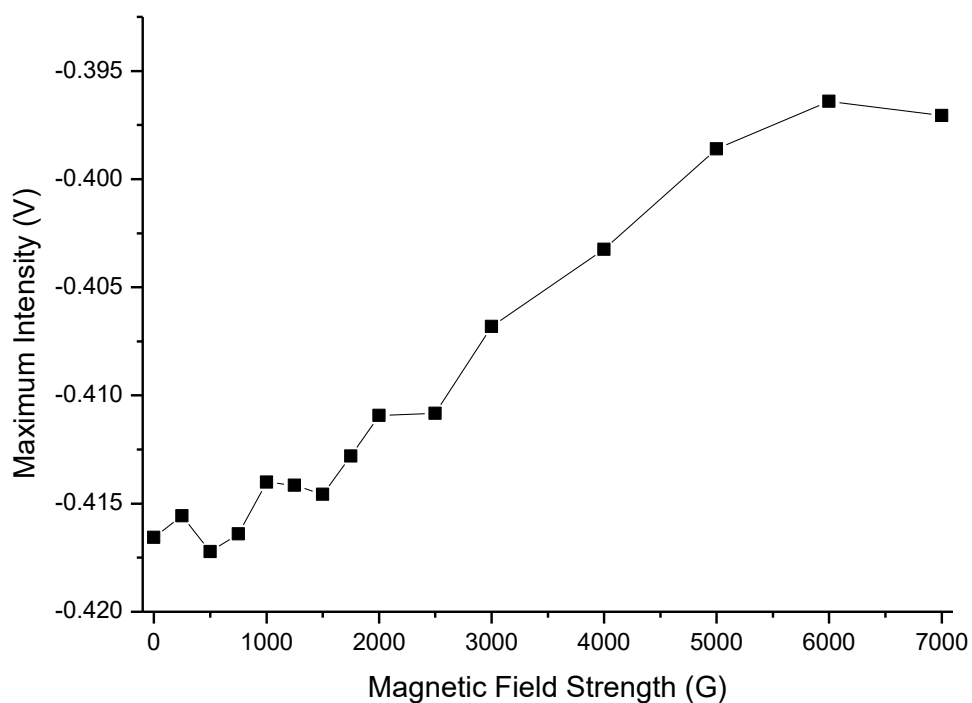


Figure 26 Delayed Fluorescence ZnTPP + perylene in mesitylene

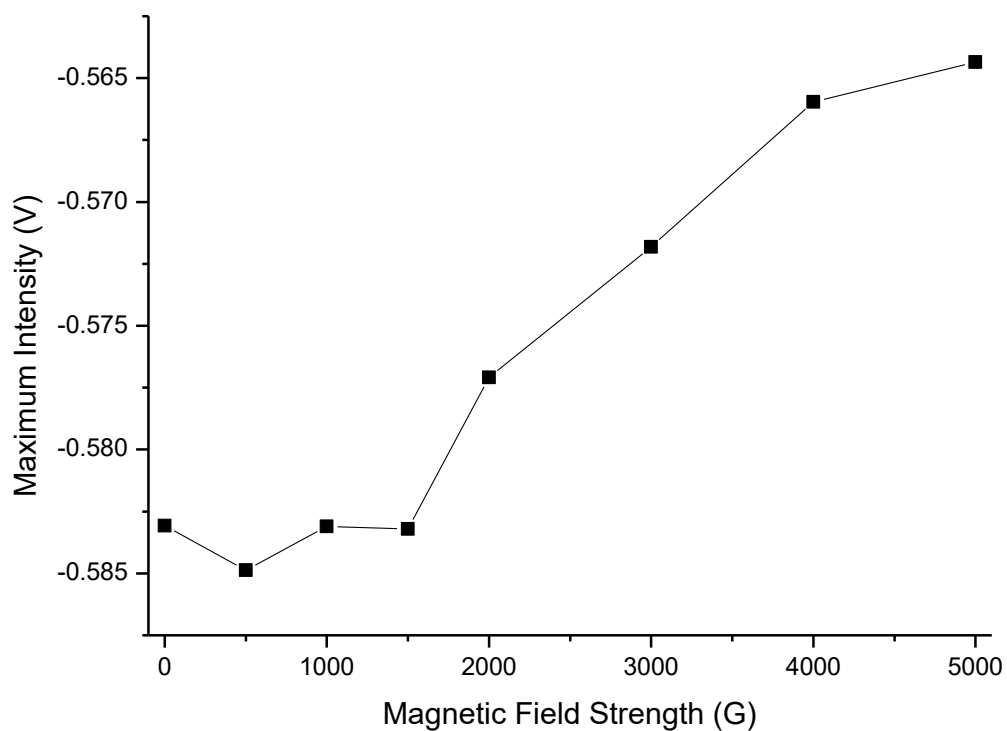


Figure 27 Delayed Fluorescence ZnTPP + perylene in octanol

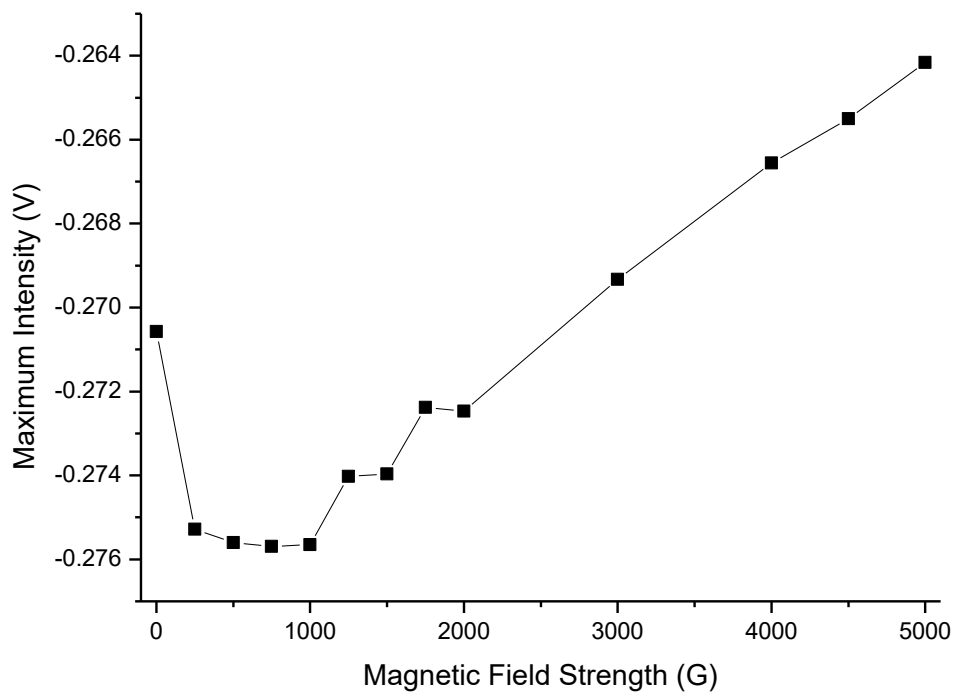


Figure 28 Delayed Fluorescence ZnTPP + perylene in paraffin oil

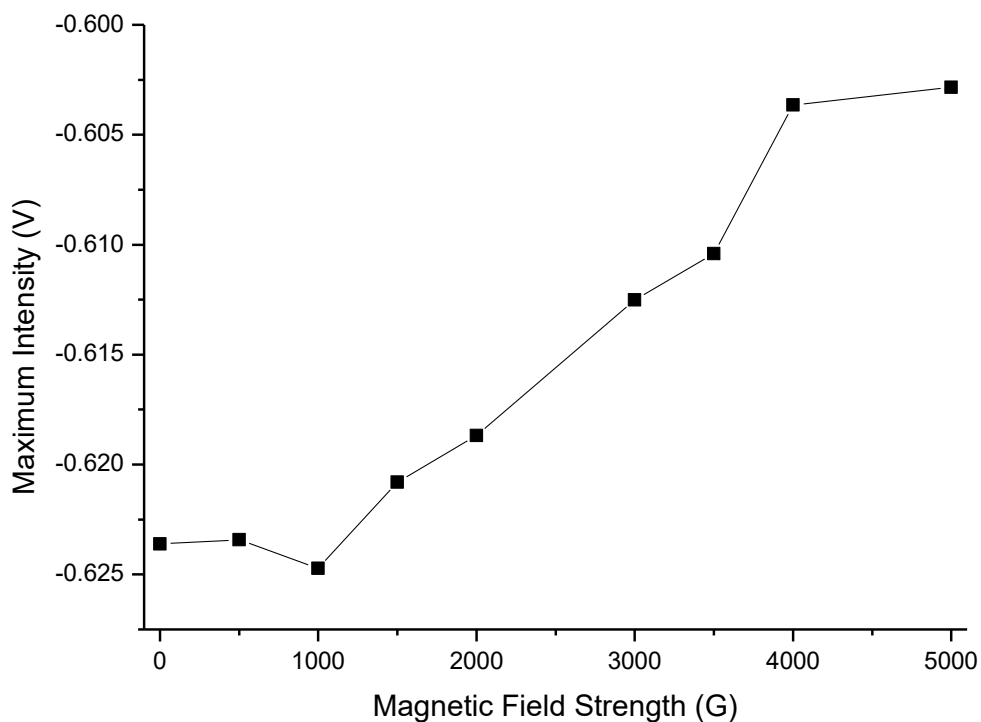


Figure 29 Delayed Fluorescence ZnTPP + perylene in toluene

All these figures prove that the magnetic field influences the delayed fluorescence intensity and show a similar behavior. This behavior will be further explained in chapter 4.2.6.

4.2.2 Viscosity Dependence

A pre-peak in front of the delayed fluorescence signal was noticed during the measurements. This pre-peak seemed to be dependent on the viscosity as it was much larger in high viscosity solvents (paraffin oil) than in low viscosity solvents (benzene).

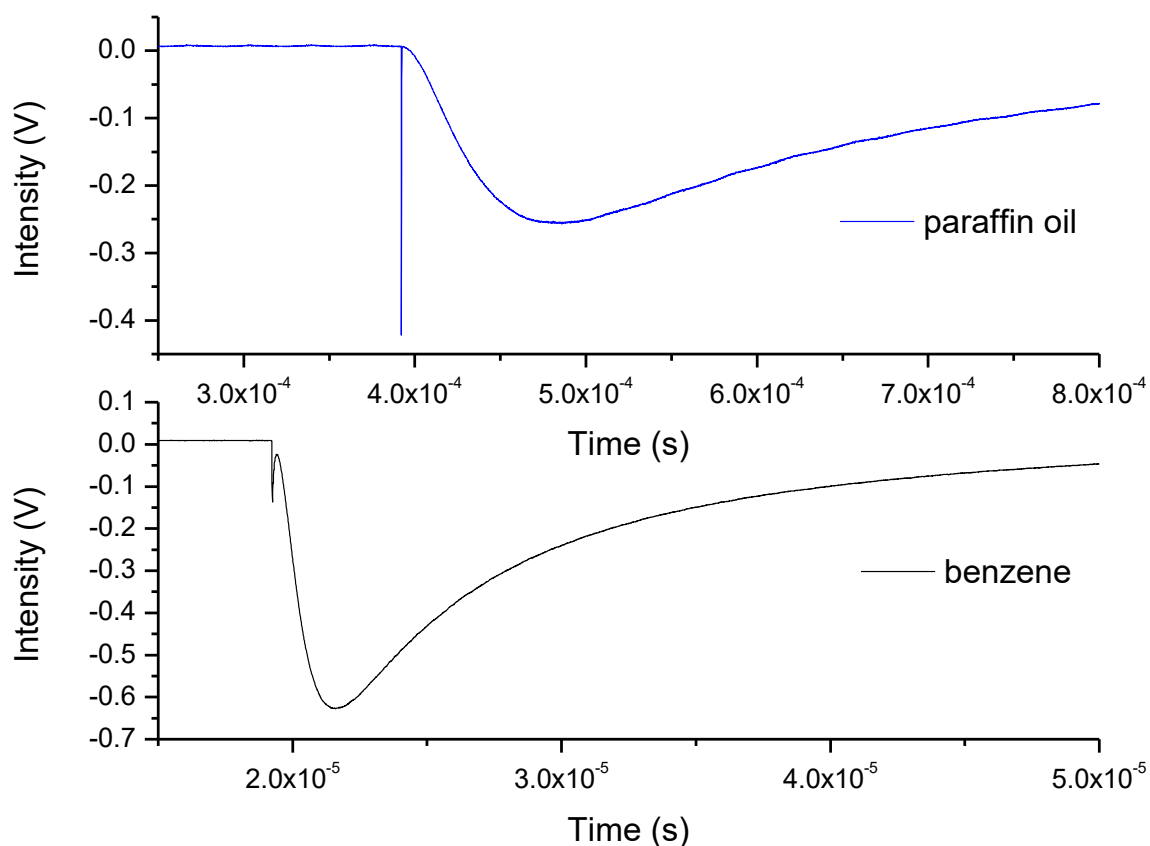


Figure 30 Pre-peak in benzene and paraffin oil with ZnTPP (1×10^{-4} M) and perylene (5×10^{-4} M)

To investigate the origin of this pre-peak a spectral analysis was performed. This means a delayed fluorescence measurement every 5-10 nm with ZnTPP and perylene in paraffin oil (as here the pre-peak is much more pronounced and easier to analyze) and octanol (as a reference in another solvent with a medium viscosity) was done and the intensity of the pre-peak plotted against the wavelength to get an idea about the fluorescence spectra. As can be seen in Figure 31 the spectra differ slightly in the two solvents.

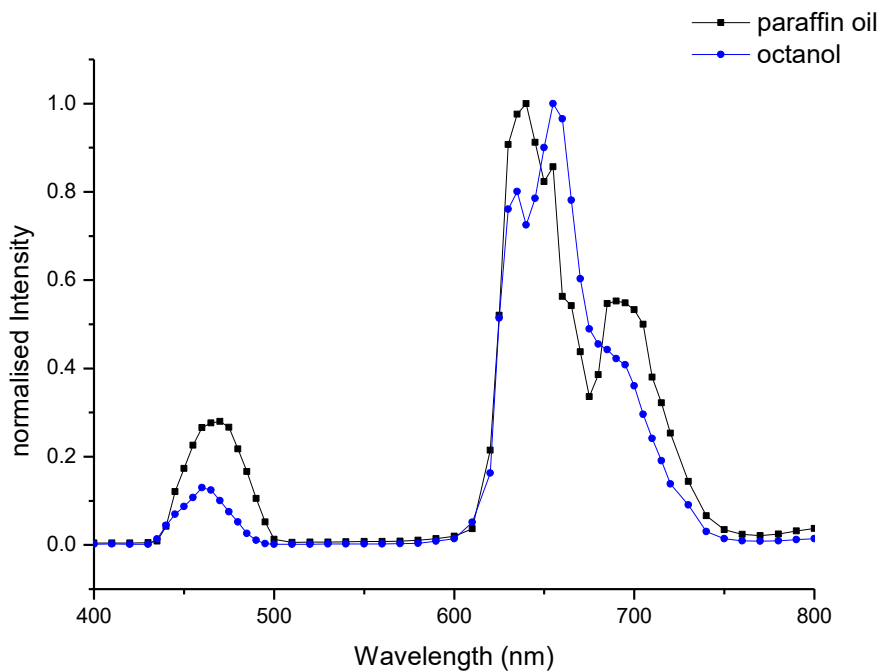


Figure 31 Spectral analysis of pre-peak in paraffin oil and octanol

Afterwards these spectra were compared to the fluorescence spectra of perylene and ZnTPP to see if they coincide.

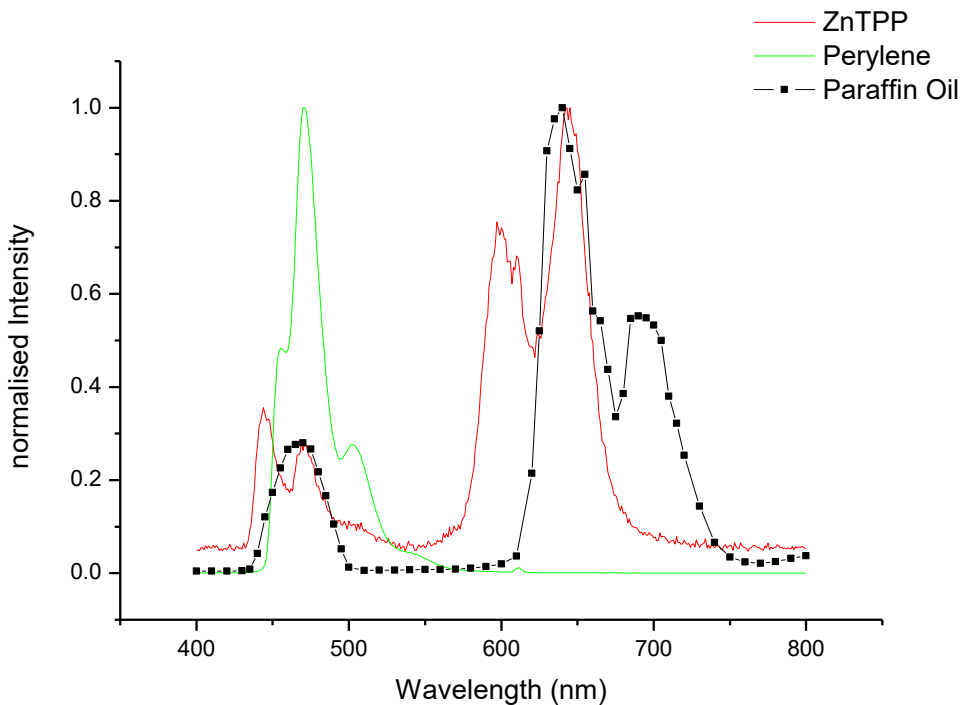


Figure 32 Spectral comparison in paraffin oil

The perylene spectrum does not fit at all while the ZnTPP spectrum is a little shifted for the last two peaks and the first peak at the black curve is split into two for the red curve, but seems to mostly fit. Therefore, the pre-peak should be from some kind of ZnTPP fluorescence.

Next, the dependence on the viscosity was analyzed using the solvent mixtures described in Table 2 Viscosity mixture composition. The following figure shows the pre-peaks of the different mixtures normalized to the maximum value of their own time dependent measured decay curve. The time axis does not show at which point in time the pre-peak showed up but only how long a pre-peak is, as the peaks are ordered there arbitrarily. The legend depicts the viscosity in cP of the mixture in the corresponding measurement.

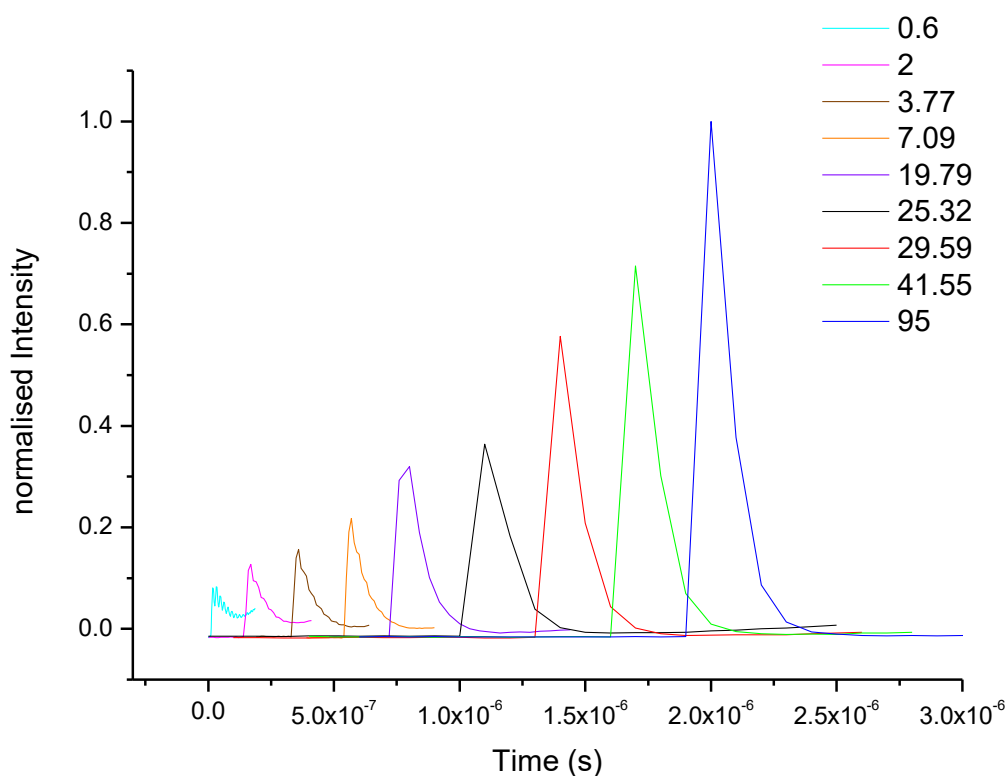


Figure 33 Pre-peak intensities at different viscosities

Figure 34 shows the maxima of the pre-peaks plotted against the viscosity. A definite trend can be seen. To make sure that this is not an effect of other solvent properties a measurement in octanol (viscosity around 7) has been performed. Octanol shows a normalized peak value

of 0.204 while the benzene and paraffin oil mixture at 7.09cP has a normalized peak value of 0.217. As such, it can be assumed that the influence is from the viscosity.

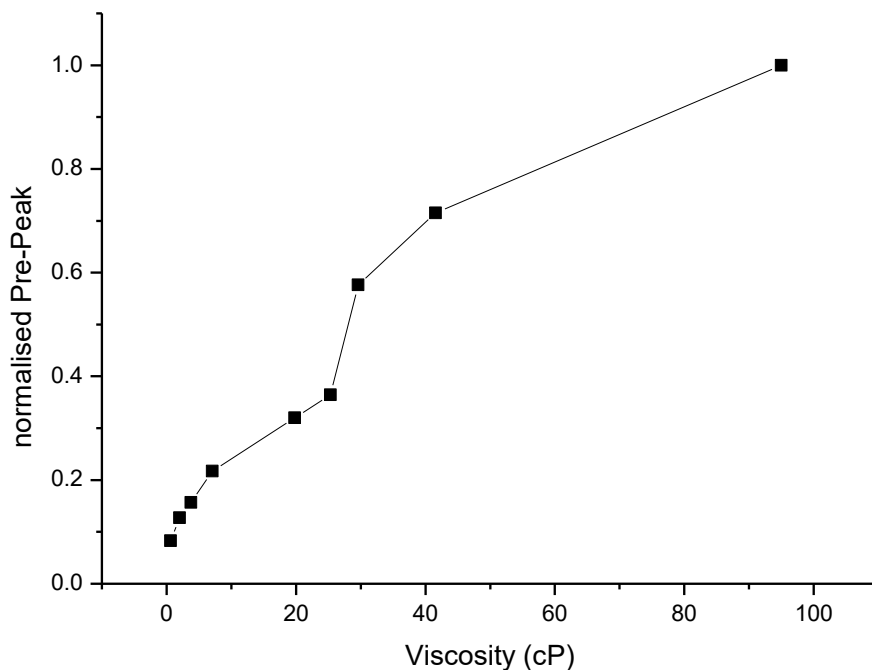


Figure 34 Viscosity dependence of pre-peak

There are no other chemicals in the sample except the solvent, which itself does not show any fluorescence in this region. The S_2 state of ZnTPP has twice the energy of the T_1 state, which means that ZnTPP can perform a self TTA reaction. This generates a S_2 and a S_0 state. The reaction has to happen before the ZnTPP triplet meets a perylene ground state, because in that case energy transfer would take place, effectively removing the ZnTPP triplet. The concentration of perylene is much higher than the concentration of ZnTPP and so the self TTA process has to happen fast, and only happens between ZnTPP triplets that are already in the vicinity of each other before the laser excitation. The viscosity dependence stems from the fact that, with lower viscosity these triplets can diffuse apart faster and are moving faster in the solvent. A higher viscosity keeps them together for a longer period of time and allows more such pairs to react with each other before diffusing apart.

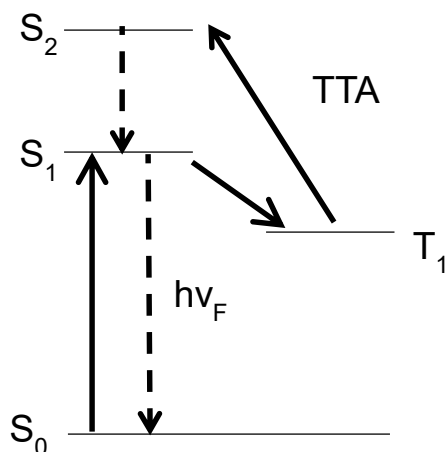


Figure 35 Energy schematic self TTA ZnTPP

From the S_2 state, the excited electrons are decaying back to the S_1 state, from which light is emitted. The short lifetime of the pre-peak, although it technically is also delayed fluorescence, can be understood by looking at the reason for the delay in delayed fluorescence. The lifetime of the triplet state is many times longer than the S_1 state and during the whole life time of the T_1 state, TTA can be performed which leads to new S_1 states. Therefore, the generation of S_1 states is not, like in normal time correlated fluorescence, only occurring during the short excitation pulse, but during the whole lifetime of the triplet. In the ZnTPP self TTA case, the TTA can only be performed right after the pulse, before diffusion starts, and as such the life time of the triplet can't be used to delay the S_1 generation and the life time of the S_2 is extremely short. As such, the lifetime of the pre-peak has to be short. This effect could not be observed when using PdTPP but with SnTPP, (see Figure 36) it was seen. For PdTPP the energy levels of the different states are known and it is not possible for PdTPP to perform a self TTA reaction. For SnTPP the energy levels are unknown, but as a pre-peak can be observed, it is highly likely that the energy levels allow a self TTA reaction.

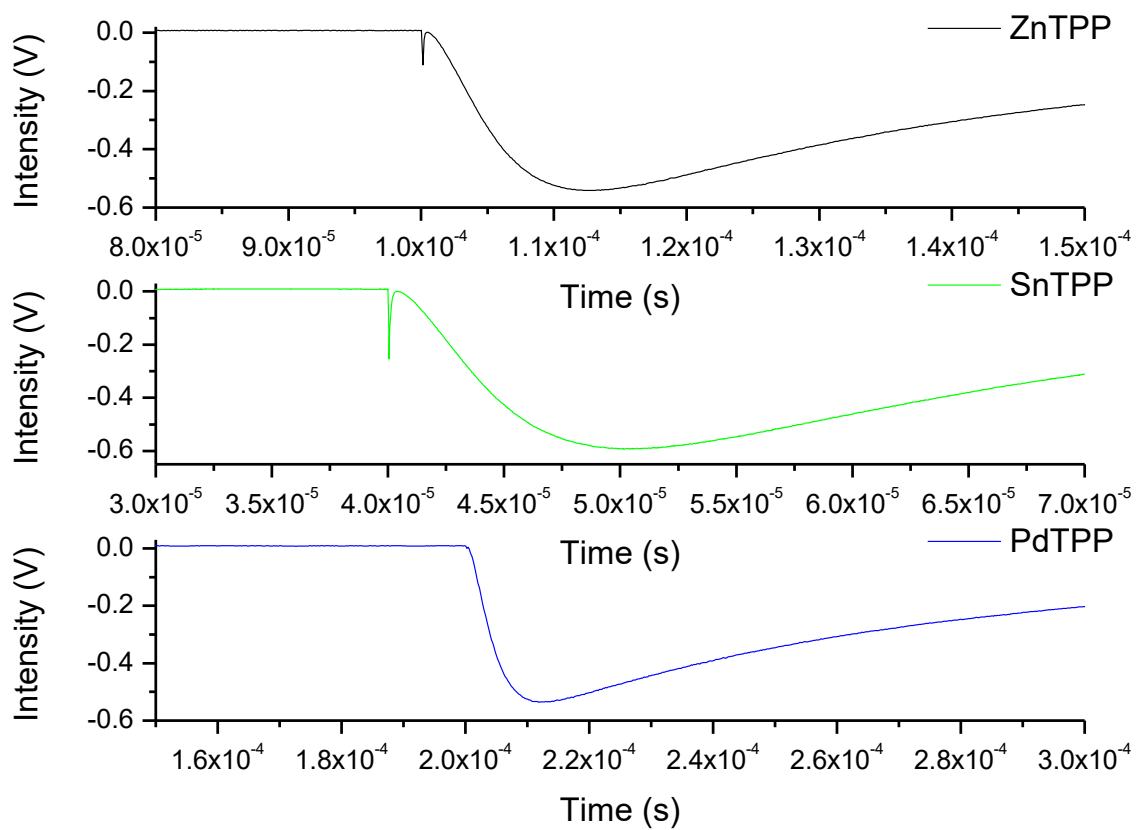


Figure 36 Delayed Fluorescence Decay Curves in Octanol

4.2.3 PdTPP and Perylene

The curves of the following three chapters will be discussed together in the conclusion chapter

4.2.6

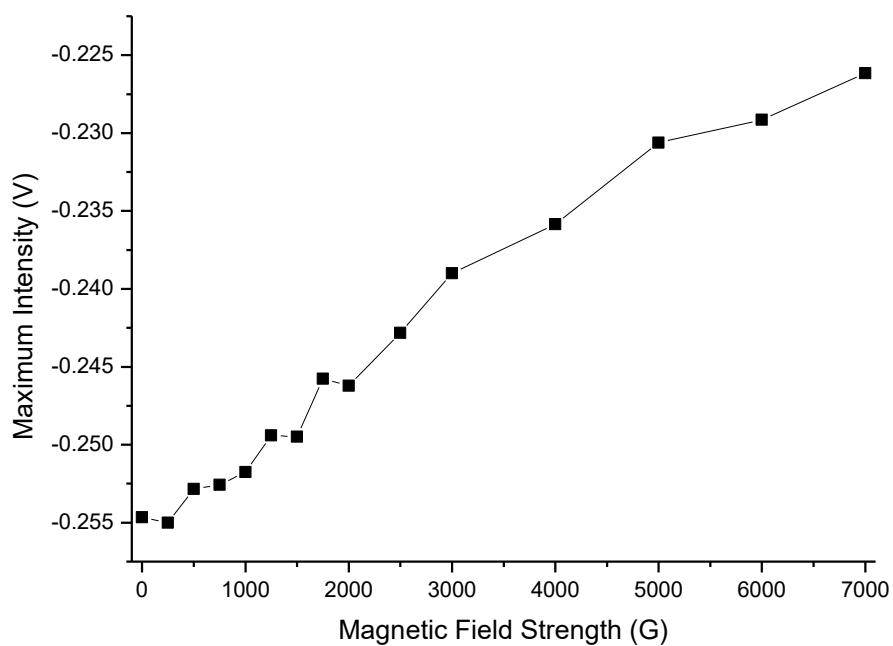


Figure 37 Delayed fluorescence PdTPP and perylene in cyrene

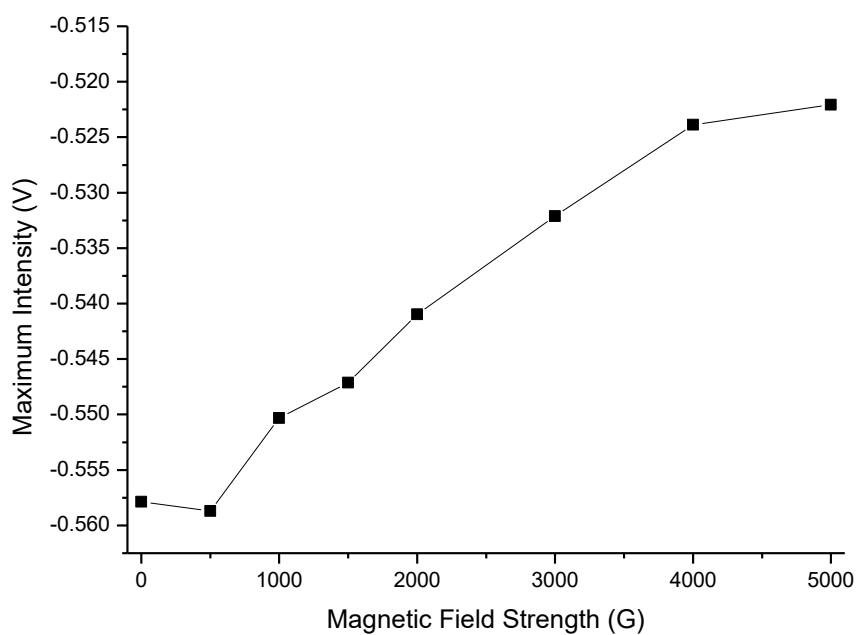


Figure 38 Delayed fluorescence PdTPP and perylene in octanol

4.2.4 SnTPP and Perylene

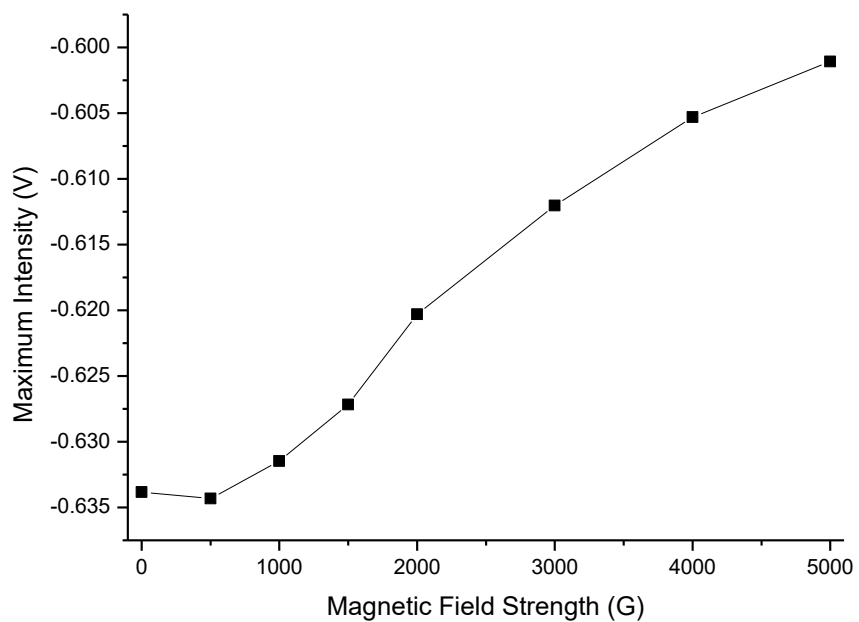


Figure 39 Delayed fluorescence SnTPP and perylene in octanol

4.2.5 Comparison different Sensitizer

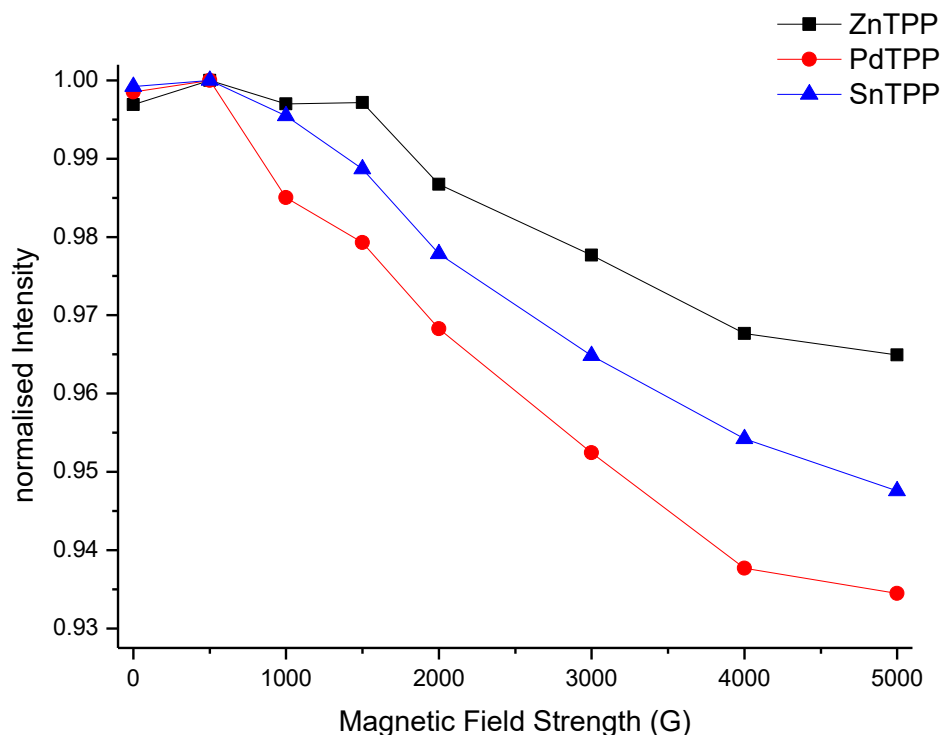


Figure 40 MFE of different Sensitizer with Perylene in Octanol

4.2.6 Conclusion

All of the three here presented sensitizer-annihilator pairs show a magnetic field effect on their intensities. The strength of this effect varies with the solvent and the sensitizer. The effect is large enough and reproducible to discount it as an artifact and it can be stated that a magnetic field influences the intensity of the delayed fluorescence reaction. At high magnetic field strength the intensity decreases, while at low magnetic field strength the intensity stays around the same value as when no field is applied or increases slightly. The magnetic field strength starting from which a decrease in the intensity can be noticed, varies with solvent and sensitizer used.

In comparison to the solid state, a slightly different behavior can be seen no noticeable increase in the intensity at low field values is experienced, but the decrease at high field values can still be observed. This is because in solution the molecules are not orientated in the same way like in the solid state, but are rather randomly orientated. As such for a few particles, the

magnetic field direction will be in resonance direction for a few in off resonance and for the rest in between. This means that only a percentage of the states, which should be available for mixing, are actually able to do so and the effect is repressed in comparison to the solid state. For this reasons the intensity stays the same at the low field. At higher field values, the spins are quantized along the external field and the behavior gets closer to the one observed in the solid state, namely a decrease in the intensity.

5 pH-dependent Transient Triplet Absorption

5.1 Measurement

At the beginning of the thesis a few, to the rest unrelated, measurements have been done in order to obtain the required degree of familiarization with the equipment. The idea was to measure Stern-Volmer plots for mixtures of eosin/erythrosine with cysteine/tryptophan in dependence of the pH value. The performed measurements were time resolved transient absorption measurements of the triplet state of eosin or erythrosine. The lifetime has been calculated from the measured data and has been used for Stern-Volmer plots for further analysis.

Lifetime calculation was done by using a first order exponential fit on the measured decay curves. The Stern-Volmer relationship [8] describes the relation between the intensity or the lifetime of a fluorophore with the concentration of a substance, that quenches this fluorescence. The following equation shows the formal relationship for the lifetime:

$$\frac{\tau_0}{\tau} = 1 + \tau_0 k_q [Q] \quad (17)$$

τ_0 = lifetime of the fluorophore without quencher

τ = lifetime of the fluorophore with quencher

k_q = quenching rate constant

[Q] = concentration of quencher

By measuring the lifetime at different quencher concentrations and without quencher, k_q can be calculated using equation (17). This is done by plotting τ_0/τ against the quencher concentration. The slope of the resulting line is then divided by τ_0 to get k_q .

For these measurements the excimer laser with 308nm has been used as an excitation source as seen in Figure 6. Observation was at 580nm for all samples. The erythrosine/eosin concentration was $2 \times 10^{-5} \text{M}$. Tryptophan ranged from $5 \times 10^{-5} \text{M}$ to $4 \times 10^{-3} \text{M}$ and cysteine from $1 \times 10^{-4} \text{M}$ to $8 \times 10^{-3} \text{M}$. A phosphate buffer with a concentration of $5 \times 10^{-2} \text{M}$ has been used. The

buffer composition was dependent on the desired pH value and can be found in the following table:

pH	HClO ₄ 0.1M [ml]	KH ₂ PO ₄ 0.1M [ml]	H ₂ O [ml]
3	45.75	204.25	250
4	5.80	244.20	250
pH	Na ₂ HPO ₄ 0.1M [ml]	KH ₂ PO ₄ 0.1M [ml]	H ₂ O [ml]
5	1.50	248.50	250
7	97.00	153.00	250
8	215.50	34.50	250
9	245.00	5.00	250
pH	Na ₂ HPO ₄ 0,1M [ml]	NaOH 0,1M [ml]	H ₂ O [ml]
10	246.30	3.70	250
11	218.30	31.70	250

Table 3 Buffer Composition

The exact pH value of each solution was measured with a pH electrode.

5.2 Results

The measurements were analyzed using a Stern-Volmer plot to then calculate the quenching rate constant (k_q). This data was then further used in order to analyze if a photoinduced electron transfer effect is the reason for the redox reactions in these amino acids.

5.2.1 Eosin & Cysteine

pH	k_q [M ⁻¹ s ⁻¹]
6.79	8.41x10 ⁶
8.62	7.41x10 ⁷
9.37	8.42x10 ⁷
10.00	6.50x10 ⁷
12.46	6.01x10 ⁷

Table 4 Eosin + Cysteine

5 PH-DEPENDENT TRANSIENT TRIPLET ABSORPTION - 5.2 RESULTS

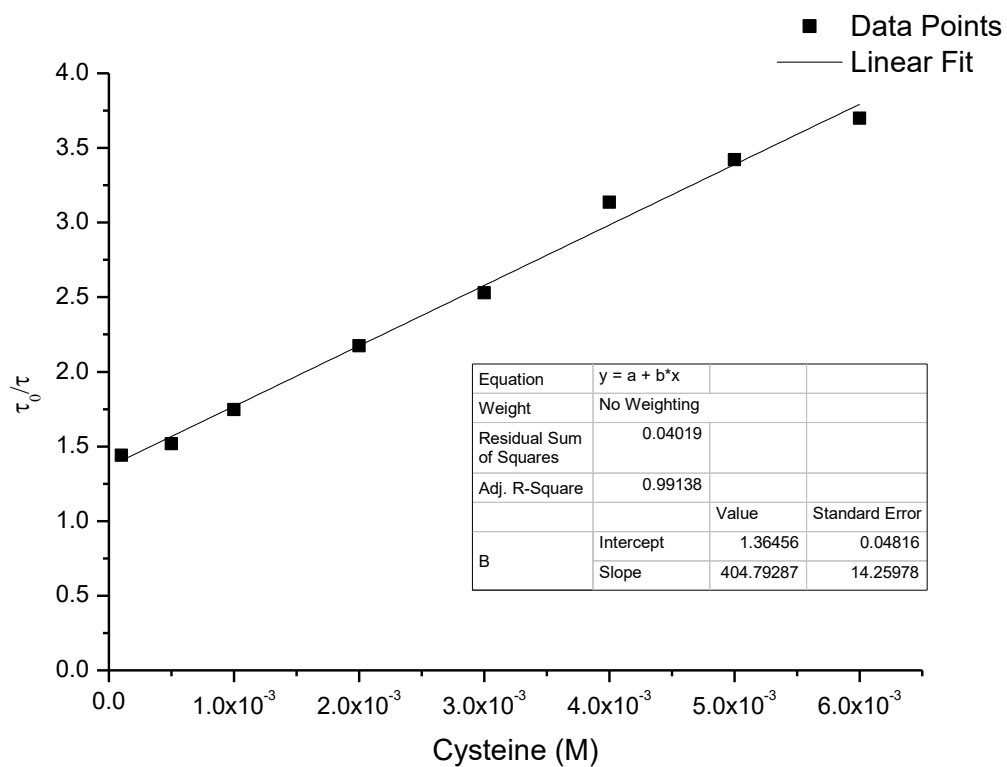


Figure 41 pH 6.79

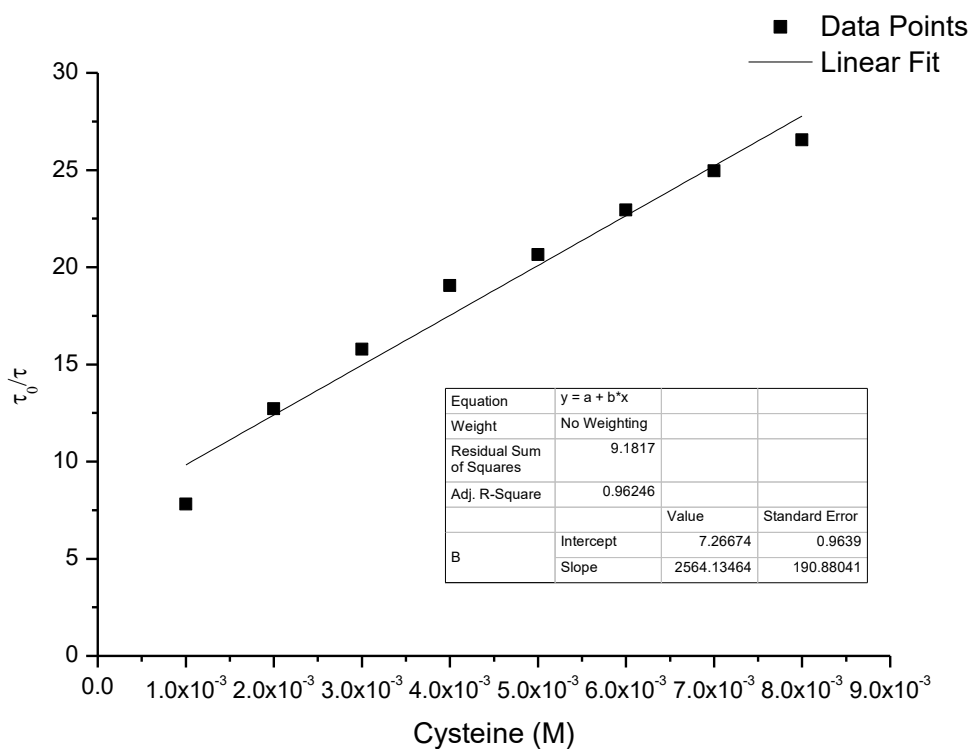


Figure 42 pH 8.62

5 PH-DEPENDENT TRANSIENT TRIPLET ABSORPTION - 5.2 RESULTS

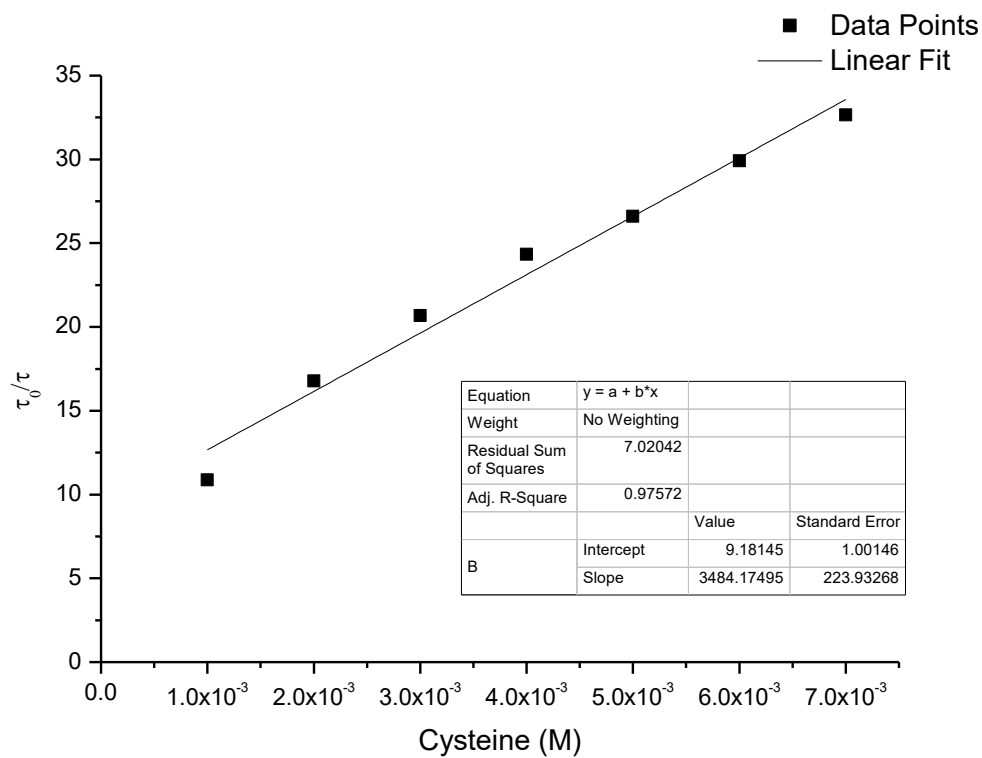


Figure 43 pH 9.37

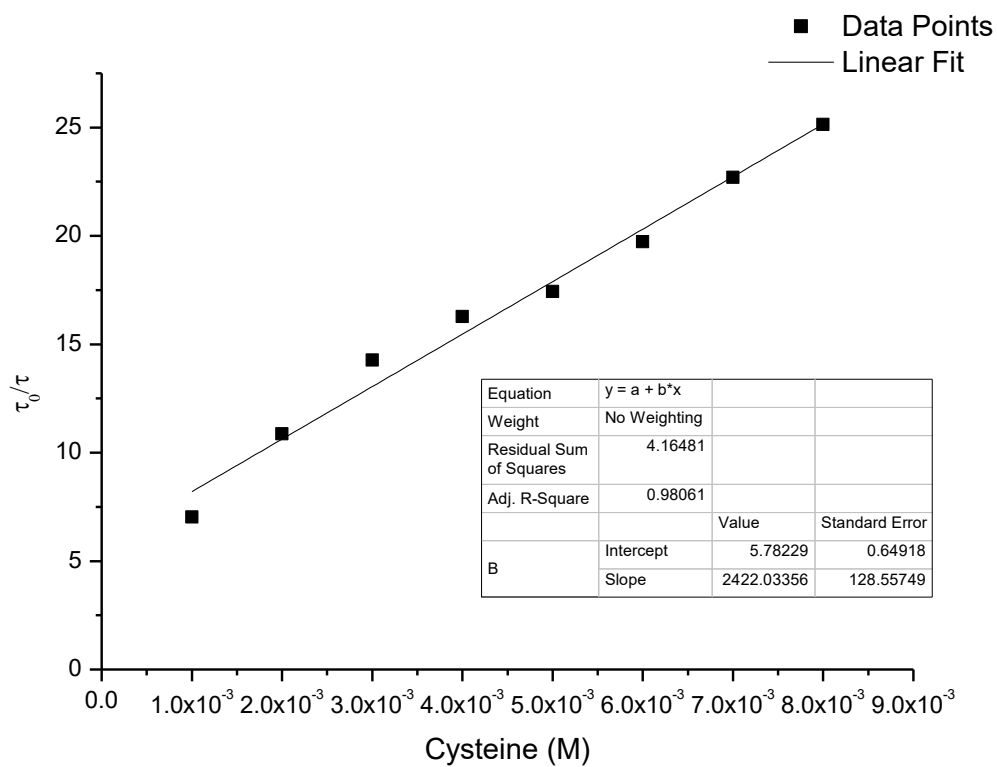


Figure 44 pH 10.00

5 PH-DEPENDENT TRANSIENT TRIPLET ABSORPTION - 5.2 RESULTS

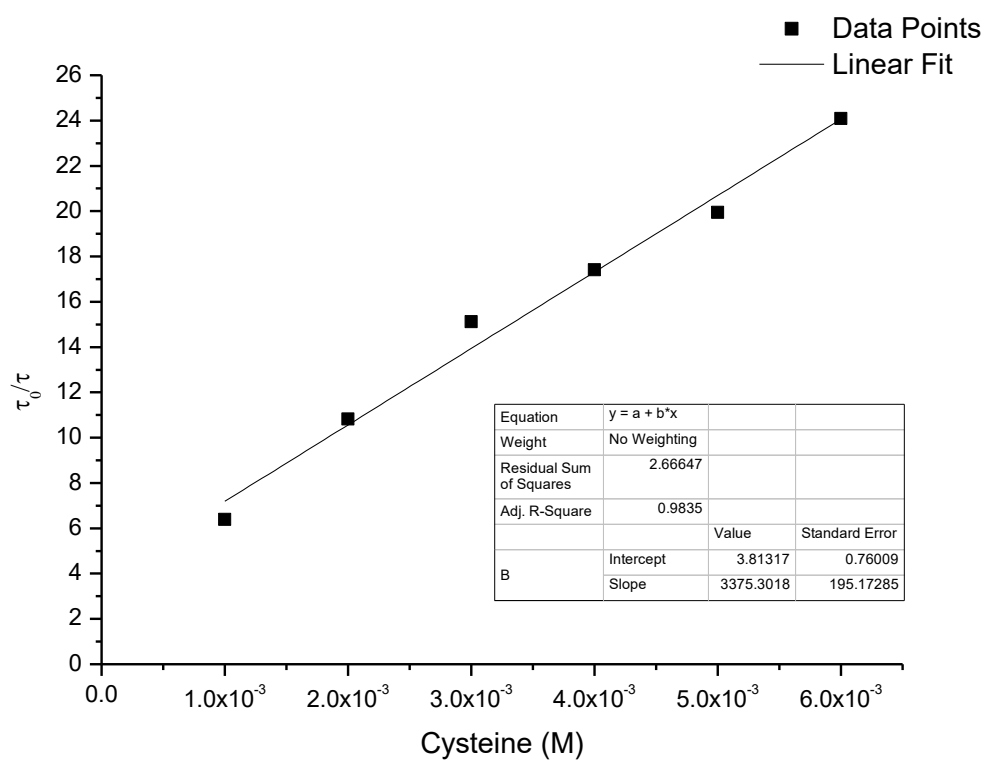


Figure 45 pH 12.46

5.2.2 Eosin & Tryptophan

pH	k_q [$M^{-1}s^{-1}$]
3.00	1.64×10^9
4.84	1.88×10^9
6.79	1.81×10^9
7.76	1.57×10^9
10.00	9.06×10^8
12.46	8.39×10^8

Table 5 Eosin + Tryptophan

5 PH-DEPENDENT TRANSIENT TRIPLET ABSORPTION - 5.2 RESULTS

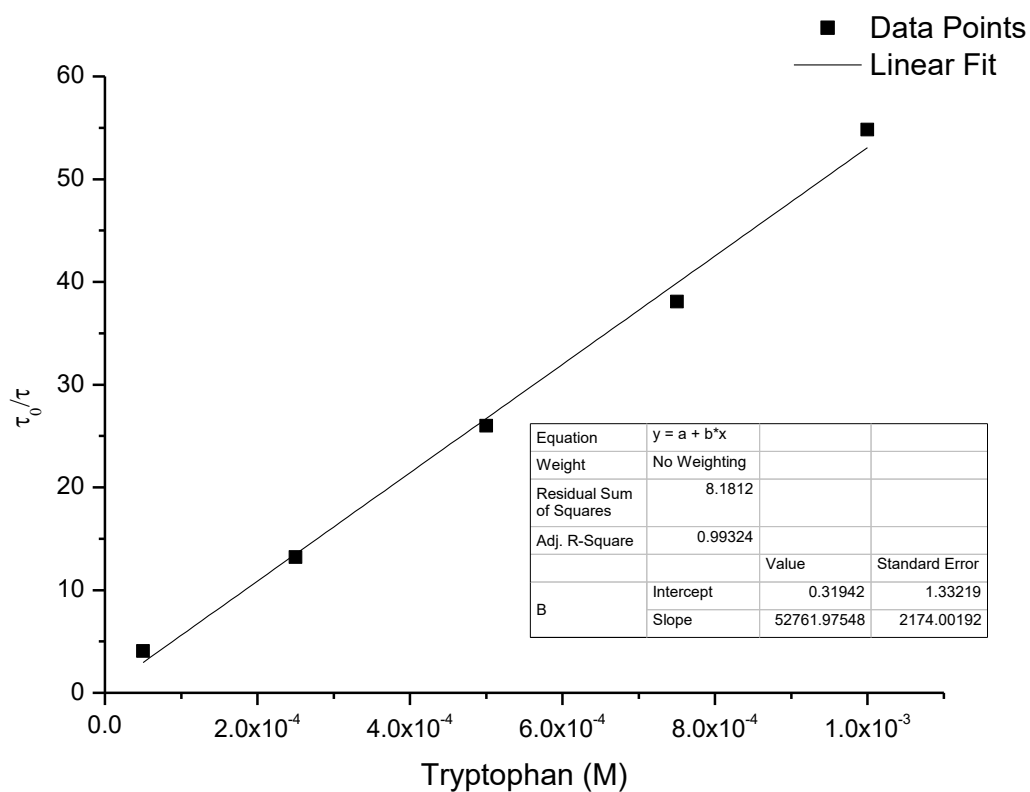


Figure 46 pH 3.00

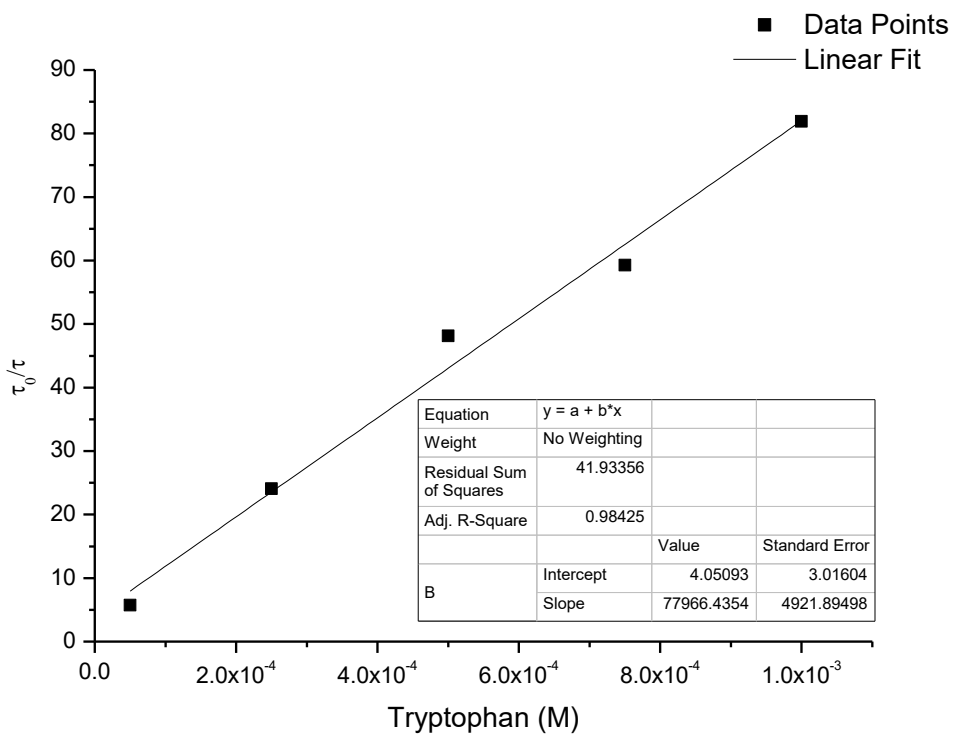


Figure 47 pH 4.84

5 PH-DEPENDENT TRANSIENT TRIPLET ABSORPTION - 5.2 RESULTS

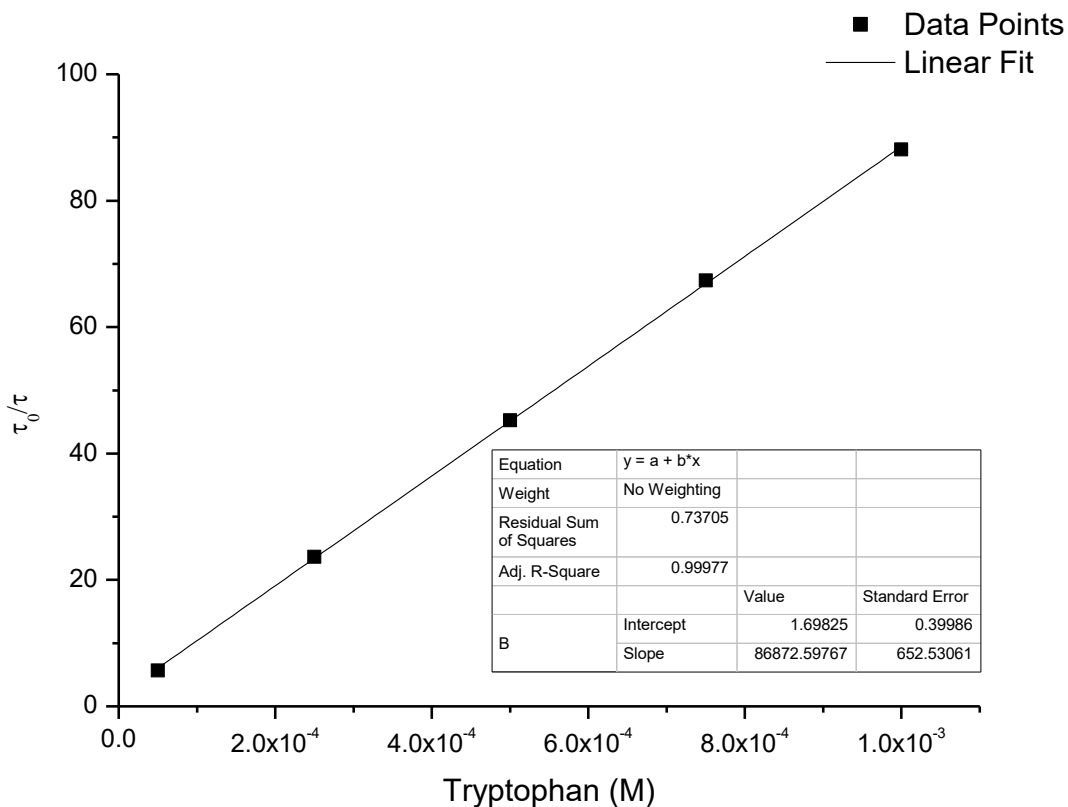


Figure 48 pH 6.79

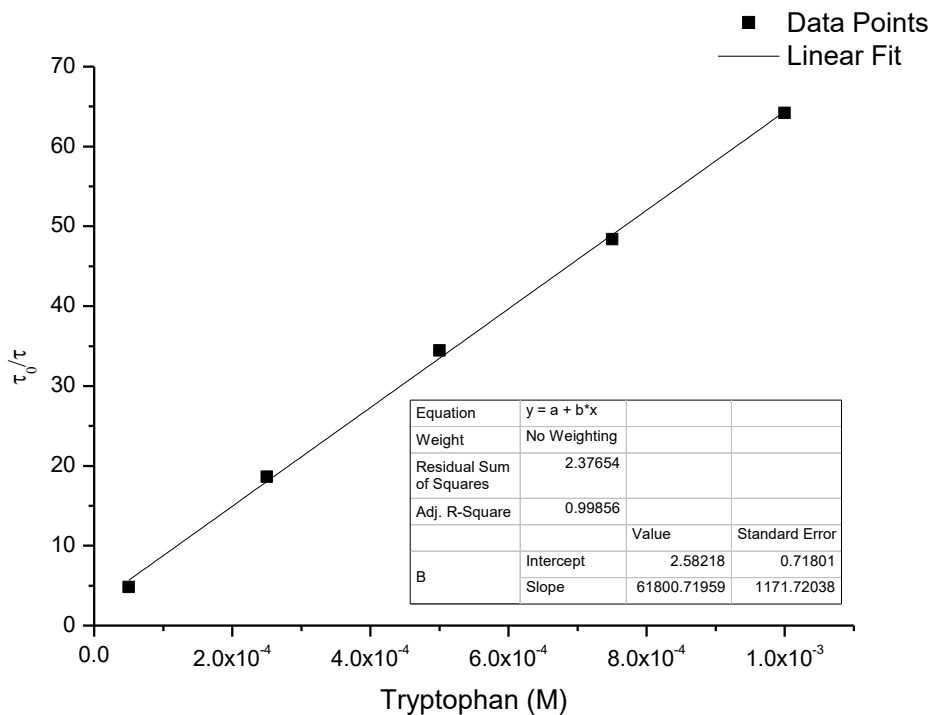


Figure 49 pH 7.76

5 PH-DEPENDENT TRANSIENT TRIPLET ABSORPTION - 5.2 RESULTS

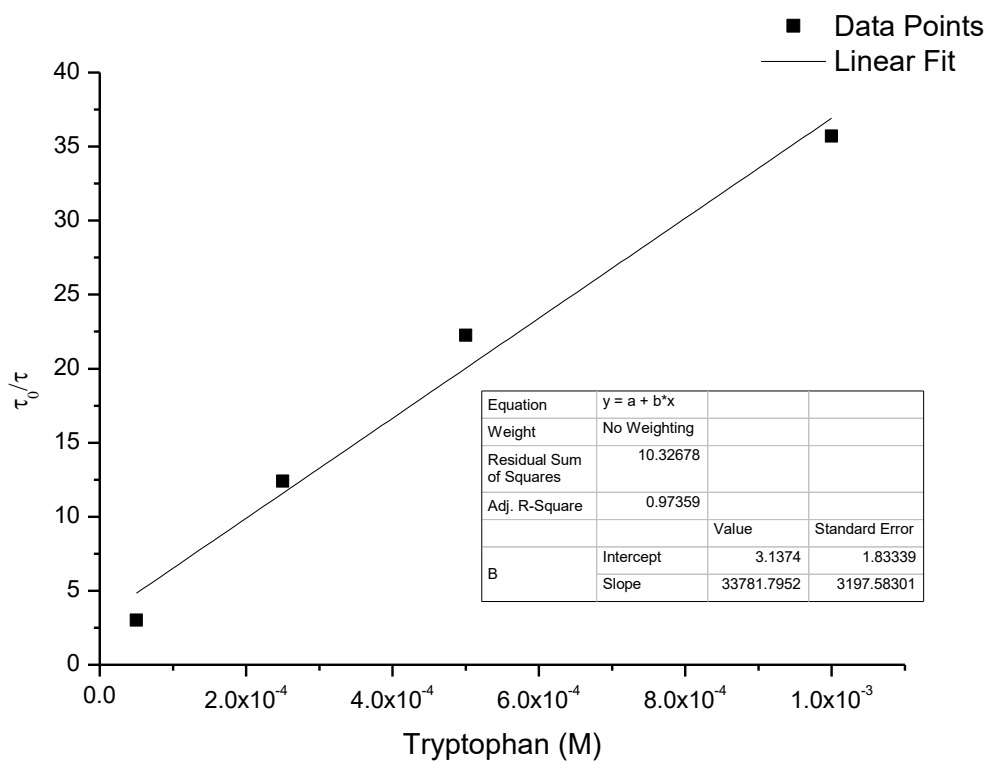


Figure 50 pH 10.00

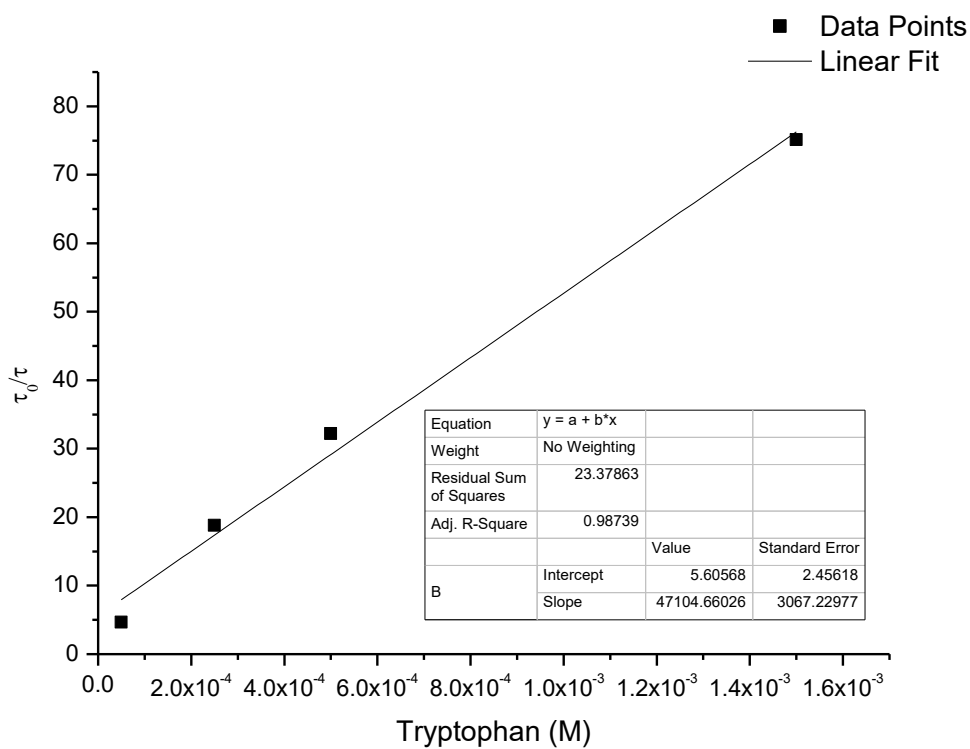


Figure 51 pH 12.46

5.2.3 Erythrosine & Cysteine

pH	k_q [$M^{-1}s^{-1}$]
7.98	4.08×10^7
10.00	7.58×10^7
12.45	1.51×10^8

Table 6 Erythrosine + Cysteine

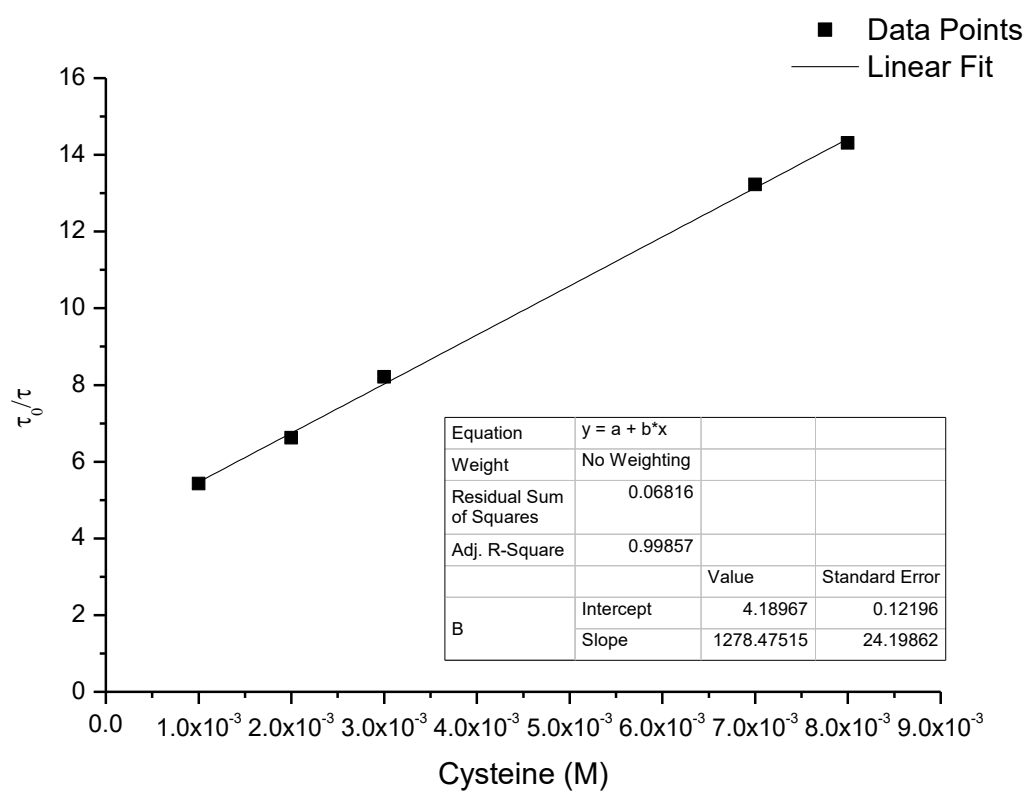


Figure 52 pH 7.98

5 PH-DEPENDENT TRANSIENT TRIPLET ABSORPTION - 5.2 RESULTS

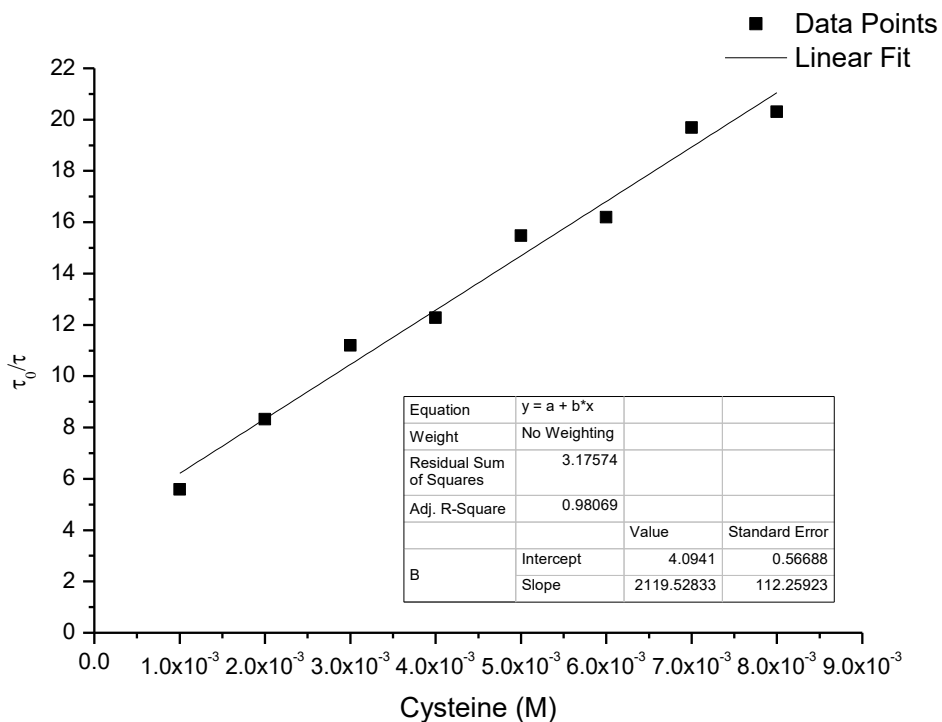


Figure 53 pH 10.00

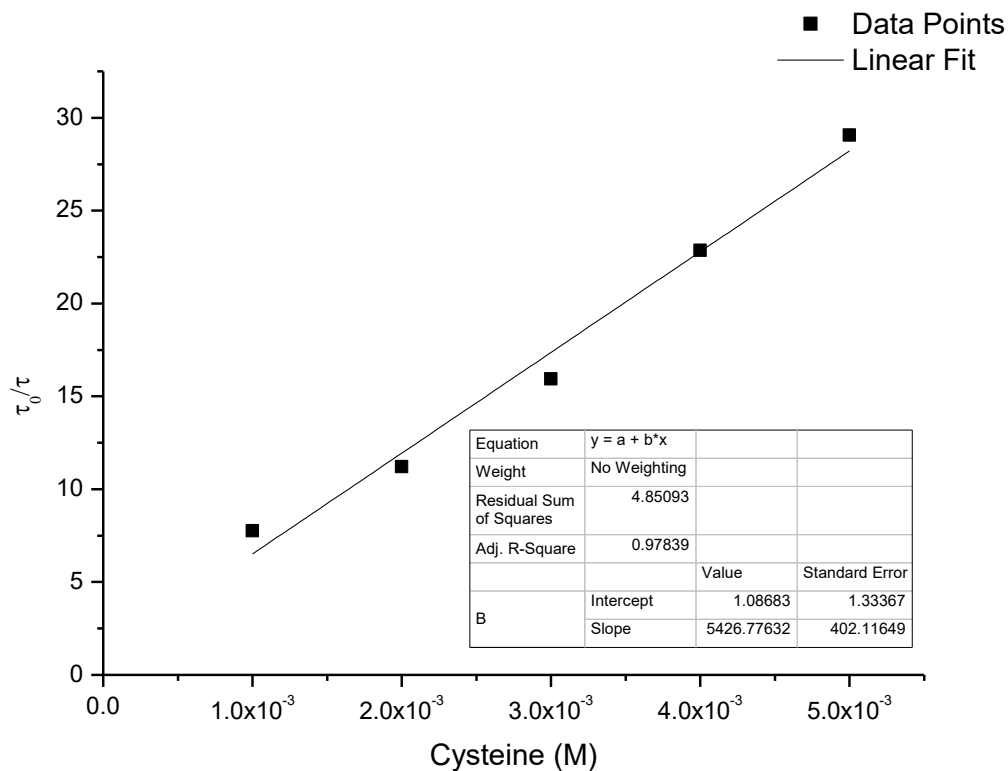


Figure 54 pH 12.45

5.2.4 Erythrosine & Tryptophan

pH	k_q [$M^{-1}s^{-1}$]
5.07	6.52×10^8
6.79	5.89×10^8
7.98	5.59×10^8
10.00	6.47×10^8
11.15	8.36×10^8

Table 7 Erythrosine + Tryptophan

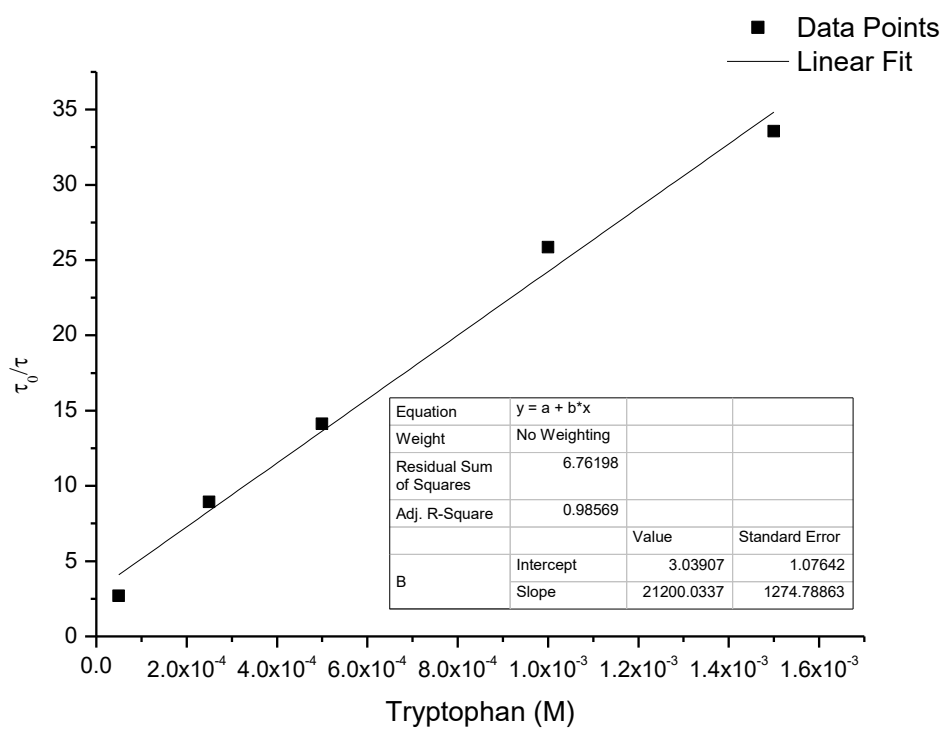


Figure 55 pH 5.07

5 PH-DEPENDENT TRANSIENT TRIPLET ABSORPTION - 5.2 RESULTS

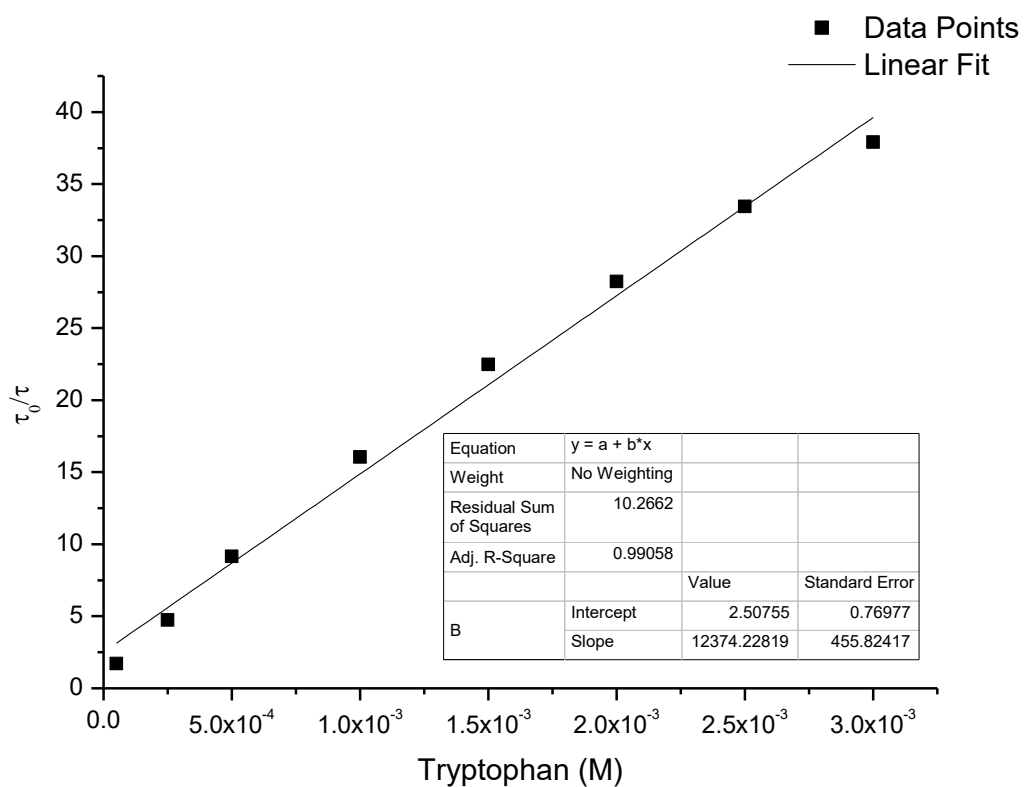


Figure 56 pH 6.79

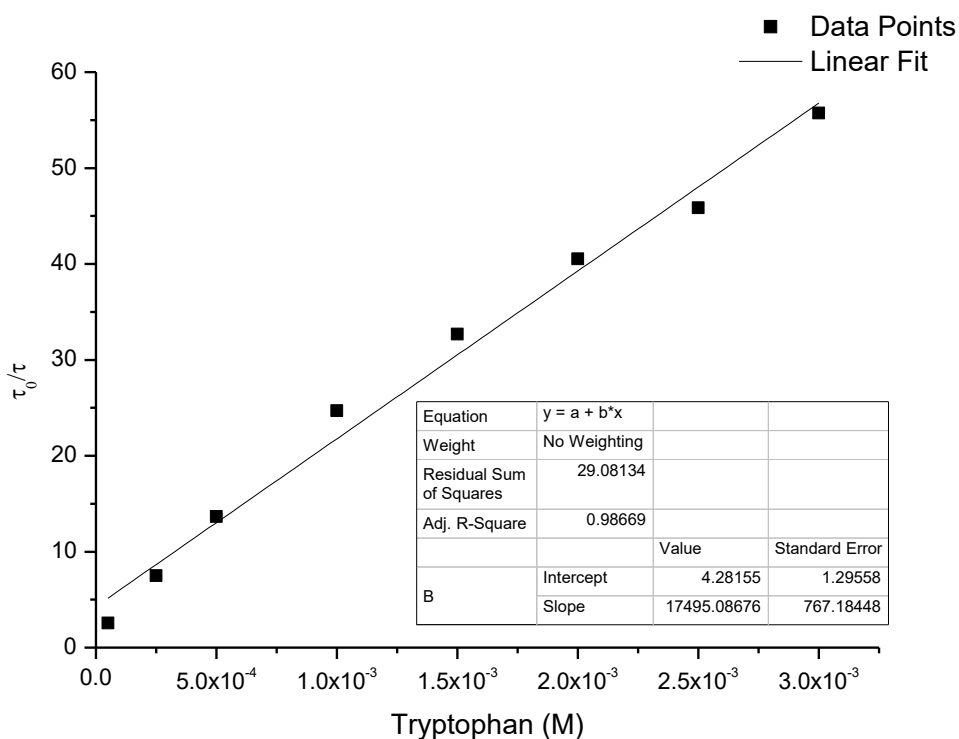


Figure 57 pH 7.98

5 PH-DEPENDENT TRANSIENT TRIPLET ABSORPTION - 5.2 RESULTS

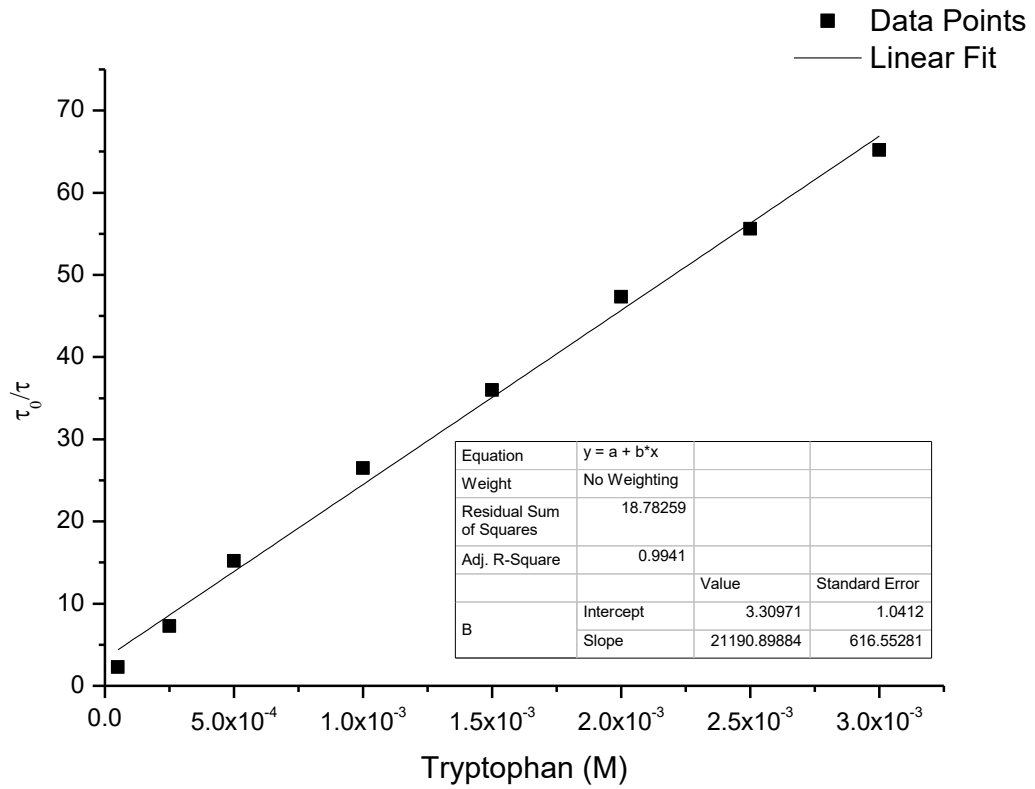


Figure 58 pH 10.00

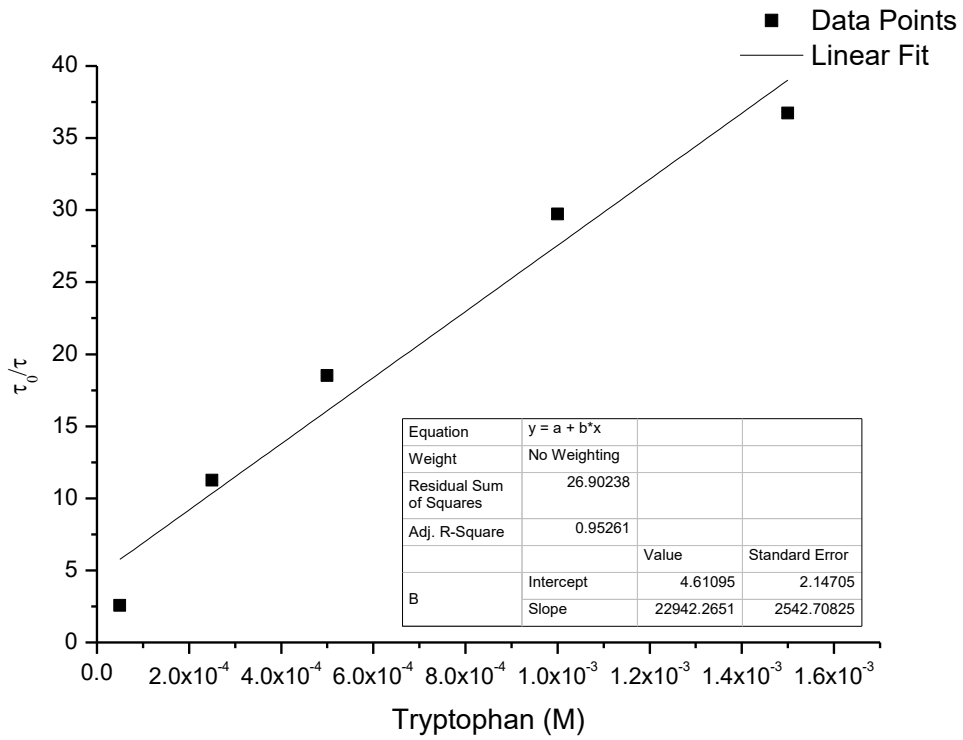


Figure 59 pH 11.15

6 Appendix

6.1 Index of Figures

Figure 1 E-Type Energy Schematic _____	2
Figure 2 P-Type Energy Schematic _____	3
Figure 3 Sensitized Delayed Fluorescence _____	4
Figure 4 Magnetic field dependence of the energy of triplet pairs for different orientations β of the magnetic field with respect to the direction perpendicular to the molecular plane for $J_Q = 1.24D$ _____	6
Figure 5 Ubbelohde Viscometer _____	10
Figure 6 Laser Setup 1 _____	12
Figure 7 Side View of Cuvette _____	12
Figure 8 Laser Setup 2 _____	13
Figure 9 Schematic Gated PMT _____	15
Figure 10 Schematic Gas Saturation _____	18
Figure 11 Concentration range measured in benzene _____	19
Figure 12 Spectra of ZnTPP and perylene in benzene _____	20
Figure 13 Spectra of PdTPP and perylene in octanol _____	21
Figure 14 Spectra of SnTPP and perylene in octanol _____	21
Figure 15 Absorption trace of ZnTPP ($1 \times 10^{-4}M$) and perylene ($5 \times 10^{-4}M$) in benzene _____	23
Figure 16 Comparison of measured and calculated decay curve of ZnTPP ($1 \times 10^{-4}M$) and perylene ($5 \times 10^{-4}M$) in benzene _____	24
Figure 17 Residuals of First Order Fit _____	24
Figure 18 Residuals for both fits _____	26
Figure 19 Dependency of Lifetime to magnetic field strength of ZnTPP ($1 \times 10^{-4}M$) and perylene ($5 \times 10^{-4}M$) in benzene _____	27
Figure 20 Emission trace of anthracene ($5 \times 10^{-4}M$) in DMF _____	28
Figure 21 Magnetic field effect anthracene ($5 \times 10^{-4}M$) in DMF _____	29
Figure 22 Delayed Fluorescence ZnTPP + perylene in acetone _____	30
Figure 23 Delayed Fluorescence ZnTPP + perylene in benzene _____	31

6 APPENDIX - 6.1 INDEX OF FIGURES

Figure 24 Delayed Fluorescence ZnTPP + perylene in cyclohexylbenzene _____	31
Figure 25 Delayed Fluorescence ZnTPP + perylene in cymene _____	32
Figure 26 Delayed Fluorescence ZnTPP + perylene in mesitylene _____	32
Figure 27 Delayed Fluorescence ZnTPP + perylene in octanol _____	33
Figure 28 Delayed Fluorescence ZnTPP + perylene in paraffin oil _____	34
Figure 29 Delayed Fluorescence ZnTPP + perylene in toluene _____	34
Figure 30 Pre-peak in benzene and paraffin oil with ZnTPP ($1 \times 10^{-4} \text{M}$) and perylene ($5 \times 10^{-4} \text{M}$) _____	35
Figure 31 Spectral analysis of pre-peak in paraffin oil and octanol _____	36
Figure 32 Spectral comparison in paraffin oil _____	36
Figure 33 Pre-peak intensities at different viscosities _____	37
Figure 34 Viscosity dependence of pre-peak _____	38
Figure 35 Energy schematic self TTA ZnTPP _____	39
Figure 36 Delayed Fluorescence Decay Curves in Octanol _____	40
Figure 37 Delayed fluorescence PdTPP and perylene in cymene _____	41
Figure 38 Delayed fluorescence PdTPP and perylene in octanol _____	42
Figure 39 Delayed fluorescence SnTPP and perylene in octanol _____	42
Figure 40 MFE of different Sensitizer with Perylene in Octanol _____	43
Figure 41 pH 6.79 _____	47
Figure 42 pH 8.62 _____	47
Figure 43 pH 9.37 _____	48
Figure 44 pH 10.00 _____	48
Figure 45 pH 12.46 _____	49
Figure 46 pH 3.00 _____	50
Figure 47 pH 4.84 _____	50
Figure 48 pH 6.79 _____	51
Figure 49 pH 7.76 _____	51
Figure 50 pH 10.00 _____	52
Figure 51 pH 12.46 _____	52
Figure 52 pH 7.98 _____	53

Figure 53 pH 10.00	54
Figure 54 pH 12.45	54
Figure 55 pH 5.07	55
Figure 56 pH 6.79	56
Figure 57 pH 7.98	56
Figure 58 pH 10.00	57
Figure 59 pH 11.15	57

6.2 Index of Tables

Table 1 Chemicals.....	9
Table 2 Viscosity mixture composition (benzene/paraffin oil)	17
Table 3 Buffer Composition.....	46
Table 4 Eosin + Cysteine	46
Table 5 Eosin + Tryptophan	49
Table 6 Erythrosine + Cysteine.....	53
Table 7 Erythrosine + Tryptophan.....	55

6.3 Index of Equations

(1)	2
(2)	3
(3)	3
(4)	4
(5)	4
(6)	4
(7)	4
(8)	4
(9)	4
(10)	7
(11)	17

(12)	17
(13)	17
(14)	17
(15)	25
(16)	25
(17)	45

6.4 Bibliography

1. **Parker, C A.** *Advances on Photochemistry*. 1964, Vol. 2, p. 305.
2. **Mezyk, J., et al.** Effect of an External Magnetic Field on the Up-Conversion Photoluminescence of Organic Films: The Role of Disorder in Triplet-Triplet Annihilation. *Physical Review Letters*. 2009, Vol. 102, 8, pp. 087404/1-087404/4.
3. **Avakian, P.** Influence of magnetic fields on luminescence involving triplet excitons. *Pure and Applied Chemistry*. 1974, Vol. 37, 1-2, pp. 1-19.
4. **Rosspointner, A.** *Experimental Observations of Diffusional Effects on Photoinduced Electron Transfer Reactions*. Graz : TU Graz, 2008. PhD Thesis.
5. **Faulkner, Larry R. and Bard, Allen J.** Magnetic field effects on anthracene triplet-triplet annihilation in fluid solutions. *Journal of the American Chemical Society*. 1969, Vol. 91, 23, pp. 6495-6497.
6. **Maples, R E.** *Petroleum Refinery Process Economics*. 2. s.l. : Pennwell Books, 2000.
7. **Bohne, C., Abuin, E. B. and Scaiano, J. C.** Characterization of the triplet-triplet annihilation process of pyrene and several derivatives under laser excitation. *Journal of the American Chemical Society*. 1990, Vol. 112, 11, pp. 4226-4231.
8. **Verhoeven, J W.** Glossary of terms used in photochemistry. *Pure and Applied Chemistry*. 1996, Bd. 68, S. 2223.
9. **Kawada, Allan and Jarangin, R C.** Delayed Ionization of Excited Phenanthrene and Anthracene in Solution. 1966, Vol. 44, 5, pp. 1919-1928.
10. **Adler, A D, et al.** On the preparation of metalloporphyrins. 1970, Vol. 32, pp. 2443-2445.
11. **Adler, Alan D, et al.** Preparation of metalloporphyrins. *J. Inorg. Nucl. Chem.* 1970, Vol. 32, 7, pp. 2443-2445.

12. **Angulo, G, et al.** Delayed Fluorescence Due to Annihilation of Triplets Produced in Recombination of Photo-Generated Ions. 2003, Vol. 107, pp. 6913-6919.
13. **Atkins, P W.** The role of electron exchange in cidep. 1979, Vol. 66, pp. 403-405.
14. **Auckett, J E, et al.** Efficient up-conversion by triplet-triplet annihilation. 2009, Vol. 185, pp. 1-4.
15. **Avakian, P, et al.** Magnetic field dependence of the triplet-triplet fusion rate constant for anthracene in solution. 1971, pp. 499-510.
16. **Balushev, Stanislav, et al.** Metal-Enhanced Up-Conversion Fluorescence: Effective Triplet-Triplet Annihilation near Silver Surface. *Nano Letters*. 2005, Vol. 5, 12, pp. 2482-2484.
17. **Bebelaar, D.** Time resolved molecular spectroscopy using high power solid state lasers in pulse transmission mode. 1974, Vol. 3, pp. 205-216.
18. **Birks, J B and Christophorou, L G.** Excimer Fluorescence. IV Solution Spectra of Polycyclic Hydrocarbons. 1964, Vol. 277, pp. 571-582.
19. **Ceroni, Paola.** Energy Up-Conversion by Low-Power Excitation: New Applications of an Old Concept. *Chemistry - A European Journal*. 2011, Vol. 17, 35, pp. 9560-9564.
20. **Charlton, J L, Dabestani, R and Saltiel, J.** Role of Triplet-Triplet Annihilation in Anthracene Dimerization. 1983, Vol. 105, pp. 3473-3476.
21. **Cheng, Yuen Yap, et al.** Kinetic Analysis of Photochemical Upconversion by Triplet-Triplet Annihilation: Beyond Any Spin Statistical Limit. *Journal of Physical Chemistry Letters*. 2010, Vol. 1, 12, pp. 1795-1799.
22. **Cheng, Yuen, et al.** On the efficiency limit of triplet-triplet annihilation for photochemical upconversion. *Physical Chemistry Chemical Physics*. 2010, Vol. 12, 1, pp. 66-71.
23. **Crouch, A M and Langford, C H.** Photophysical behaviour of zinc tetraphenylporphyrins in solutions and polymer films. 1990, Vol. 52, pp. 55-64.
24. **Faulkner, Larry R. and Bard, Allen J.** Wurster's blue cation as an anthracene triplet quencher in fluid solution and the effect of magnetic field on this interaction. *Journal of the American Chemical Society*. 1969, Vol. 91, 23, pp. 6497-6498.
25. **Gehring, Miriam and Nickel, Bernhard.** Delayed Excimer Fluorescence of Fluoranthene Due to Triplet-Triplet Annihilation. 2001, Vol. 215, 3, pp. 343-376.

26. **Gorman, D S and Connolly, J S.** A Method for Computer Analysis of Kinetics of Competing First- and Second-Order Reactions. 1973, Vol. 5, pp. 977-989.
27. **Hüttmann, G and Staerk, H.** Delayed Luminescence of Naphthalene in Isooctane. Spectral, Lifetime, and Magnetic Field Studies of Delayed Fluorescence and Monomer Phosphorescence at 293 K. 1991, Vol. 95, pp. 4951-4954.
28. **Inoue, A, et al.** Excimer and Monomer Defect Emissions of Perylene and Pyrene Crystals as Studied by the Nanosecond Time-resolved Spectroscopy Technique. 1972, Vol. 45, pp. 720-725.
29. **Islangulov, Radiy R., et al.** Noncoherent Low-Power Upconversion in Solid Polymer Films. *Journal of the American Chemical Society*. 2007, Vol. 129, 42, pp. 12652-12653.
30. **Johnson, R C and Merrifield, R E.** Effects of Magnetic Fields on the Mutual Annihilation of Triplet Excitons in Anthracene Crystals. 1970, Vol. 1, pp. 896-902.
31. **Katoh, R, et al.** Origin of the stabilization energy of perylene excimer as studied by fluorescence and near-IR transient absorption spectroscopy. 2001, Vol. 145, pp. 23-34.
32. **Kikuchi, K, Kokubun, H and Koizumi, M.** Studies on the Delayed Fluorescence by Means of a Flash Technique. 1968, Vol. 41, pp. 1545-1551.
33. **Lan, M, et al.** Absorption and EPR spectra of some porphyrins and metalloporphyrins. 2007, Vol. 74, pp. 357-362.
34. **Langelaar, J, Rettschnick, R P and Hoijtink, G J.** Studies on Triplet Radiative Lifetimes, Phosphorescence, and Delayed Fluorescence Yields of Aromatic Hydrocarbons in Liquid Solutions. 1971, Vol. 54, pp. 1-7.
35. **Lendi, K, Gerber, P and Labhart, H.** Influence of a magnetic field in delayed fluorescence of aromatic hydrocarbons in solution II. 1976, Vol. 18, pp. 449-468.
36. —. Influence of a magnetic field in delayed fluorescence of aromatic hydrocarbons in solution III. 1977, Vol. 20, pp. 145-151.
37. **Liu, Don K.K. and Faulkner, Larry R.** Delayed fluorescence efficiencies of anthracene and phenanthrene. *Journal of the American Chemical Society*. 1978, Vol. 100, 9, pp. 2635-2639.
38. **Mani, Tomoyasu and Vinogradov, Sergei A.** Magnetic Field Effects on Triplet-Triplet Annihilation in Solutions: Modulation of Visible/NIR Luminescence. *Journal of Physical Chemistry Letters*. 2013, Vol. 4, 17, pp. 2799-2804.

39. **Marsh, D F and Mink, L M.** Microscale Synthesis and Electronic Absorption Spectroscopy of Tetraphenylporphyrin H₂(TPP) and Metalloporphyrins ZnII(TPP) and NiII(TPP). 1996, Vol. 73, pp. 1188-1190.
40. **McGimpsey, W G, et al.** Delayed Fluorescence from triplet-triplet annihilation in solution. Is the T₂ state involved? 1989, Vol. 161, 4, pp. 342-346.
41. **Merrifield, R.E.** Magnetic effects on triplet exciton interactions. *Pure and Applied Chemistry*. 1971, Vol. 27, 3, pp. 481-498.
42. **Monguzii, A, Tubino, R and Meinardi, F.** Diffusion Enhanced Upconversion in Organic Systems. 2008, pp. 1-5.
43. **Moore, G F and Munro, I H.** Temperature dependence of the delayed fluorescence from pyrene solutions. 1967, Vol. 28, pp. 1291-1298.
44. **Nickel, B and Klemp, D.** The lowest triplet state of azulene-h₈ and azulene-d₈ in liquid solution. 1993, Vol. 174, pp. 297-318.
45. **Parker, C A.** Delayed fluorescence from naphthalene solutions. 1963, Vol. 19, pp. 989-994.
46. **Parker, C A and Hatchard, C G.** Delayed Fluorescence of Pyrene in Ethanol. 1963, Vol. 59, pp. 284-295.
47. **Parker, C A and Joyce, T A.** Formation Efficiency and Energy of the Perylene Triplet. 1966, pp. 108-109.
48. **Parker, C A, Hatchard, C G and Joyce, T A.** P-Type Delayed Fluorescence from Ionic Species and Aromatic Hydrocarbons. 1964, Vol. 14, pp. 311-319.
49. **Parker, C A.** Transient Effects in Triplet-Triplet Annihilation. 1964, Vol. 60, pp. 1998-2008.
50. **Parker, Cecil Allen and Joyce, Thelma A.** Delayed fluorescence of anthracene and some substituted anthracenes. *Chemical Communications (London)*. 1967, 15, pp. 744-745.
51. **Pavlopoulos, T G.** Triplet-triplet absorption and polarization spectra of anthracene. 1991, Vol. 47A, pp. 517-518.
52. **Pekkarinen, L and Linschitz, H.** Studies on Metastable States of Porphyrins. 11. Spectra and Decay Kinetics of Tetraphenylporphine, Zinc Tetraphenylporphine and Bacteriochlorophyll. 1960, Vol. 82, pp. 2407-2411.

53. **Singh-Rachford, Tanya N. and Castellano, Felix N.** Photon upconversion based on sensitized triplet-triplet annihilation. *Coordination Chemistry Reviews*. 2010, Vol. 254, 21-22, pp. 2560-2573.
54. **Spichtig, J, Bulska, H and Labhart, H.** Influence of a magnetic field in delayed fluorescence of aromatic hydrocarbons in solution I. 1976, Vol. 15, pp. 279-293.
55. **Steiner, Ulrich E. and Ulrich, Thomas.** Magnetic field effects in chemical kinetics and related phenomena. *Chemical Reviews (Washington, DC, United States)*. 1989, Vol. 89, 1, pp. 51-147.
56. **Sugunan, S K.** *Photophysical Studies of Metalloporphyrins for Sensitized Noncoherent Photon Upconversion*. [ed.] University of Saskatchewan. Saskatoon : s.n., 2012. PhD Thesis.
57. **Syage, J A.** A vector model for the role of the exchange interaction. 1982, Vol. 91, pp. 378-382.
58. **Tahara, H, et al.** Photoinduced electron-transfer reactions and magnetic field effects on the decay rates of a photogenerated biradical from zinc porphyrin–viologen linked compounds in an ionic liquid. 2012, Vol. 524, pp. 42-48.
59. **Tfibel, F and Lindqvist, L.** Excited singlet yield in T-T annihilation. A comparative study of naphthalene and anthracene in solution. 1975, Vol. 10, pp. 471-478.
60. **Tripathy, U, et al.** Photophysics of Soret-Excited Tetrapyrroles in Solution. I. Metalloporphyrins: MgTPP, ZnTPP, and CdTPP. 2008, Vol. 112, pp. 5824-5833.
61. **Verdieck, James F. and Mau, Albert W.H.** Double-photon absorption and delayed fluorescence of some aromatic hydrocarbons in solution. *Journal of Chemical Physics*. 1970, Vol. 53, 10, pp. 4108-4109.
62. **Walters, V A, et al.** Electronic Structure of Triplet States of Zinc(II) Tetraphenylporphyrins. 1995, Vol. 99, pp. 1166-1171.
63. **Wrobel, D, Lukasiewicz, J and Manikowski, H.** Fluorescence quenching and ESR spectroscopy of metallic porphyrins in the presence of an electron acceptor. 2003, Vol. 58, pp. 7-18.
64. **Wyrsh, D and Labhart, H.** Magnetic field effects in p-type delayed fluorescence of 1,2-benzanthracene in solution. 1971, Vol. 8, 2, pp. 217-219.

65. **You, Z, Hsu, C and Fleming, G R.** Triplet-triplet energy-transfer coupling: Theory and calculation. 2006, Vol. 124, pp. 1-9.